A padding method to reduce edge effects for enhanced damage identification using wavelet analysis

Elsevier Editorial System(tm) for Mechanical Systems and Signal Processing
Manuscript Draft

Manuscript Number: MSSP13-653R2

Title: A PADDING METHOD TO REDUCE EDGE EFFECTS FOR ENHANCED DAMAGE IDENTIFICATION USING WAVELET ANALYSIS

Article Type: Full Length Article

Keywords: border distortions; padding method; false indication; vibration-based damage identification; continuous wavelet transform; cracked beam.

Corresponding Author: Prof. A. Spagnoli, Ph.D.

Corresponding Author's Institution: University of Parma

First Author: Lorenzo Montanari

Order of Authors: Lorenzo Montanari; Biswajit Basu; A. Spagnoli, Ph.D.; Brian M Broderick

Revised version, June 2014

A PADDING METHOD TO REDUCE EDGE EFFECTS FOR ENHANCED DAMAGE IDENTIFICATION USING WAVELET ANALYSIS

Lorenzo MONTANARI, Biswajit BASU, Andrea SPAGNOLI, Brian M. BRODERICK

Reviewer #1

The idea of the authors seems closer to the self-minimization method described in [17] but they compare their method to easiest one (isomorphism). The authors must justify this.

Although both the proposed polynomial padding method and Messina's self-minimization method aim at searching smooth extensional functions, they are based on different algorithms (incidentally the proposed algorithm is easier to be implemented and has a lower computational cost).

The authors tried to test Messina's self-minimization method but they found it not as robust and effective as Messina's isomorphism methods. In addition, they followed the conclusions reported in Ref. [17], where Messina himself recommends to adopt isomorphism methods.

A sentence has been added in Section 4 of the revised version to explain this point.

This reviewer suggests to mention a signal-to-noise ratio such as 10log10(maxabssignal/std) in place of SNR (eqs. 9, 10). This to make straightforward the comparison to previous analyses.

The authors agree with the Reviewer that different 10log10 measurements of noise can be adopted. By considering a signal-to-noise ratio SNR* defined as 10log10(max|signal|/std_of_noise) in place of SNR of Eqs 9,10, we have: SNR=120dB corresponds to about SNR*=63dB, SNR=100dB to SNR*=53dB, SNR=80dB to SNR*=43dB and so on.

A sentence has been added in the revised version to explain this point.

The authors must consider in their simulations that a signal to noise ratio (10log10(maxabssignal/std)) in even accurate measurements cannot be higher than ~80-90 dB or, at least this reviewer never was able to make more accurate measurements.

Given the correspondence between SNR and SNR* stated in the previous point, the values of signal-to-noise ratio being considered in the simulations seem to be realistic of actual measurements.

The authors must better justify the choice connected with parameters beta1 and beta2 (eqs. 11.1-2).

There is not an unique choice with the parameters beta1 and beta2, as they depends on the features of the signal and on the noise level. Some heuristic

rules are followed. The sentence after Eq. 11 has slightly been modified to better explain these rules.

All figures related to wavelet analysis (for example fig. 5 d-f etc) must clearly mention the amount the authors are showing. This would improve the intelligibility; for example figures 8.a-d look like third derivatives but this is not clear what they are.
The quantities being presented in Figs 5-9 are stated in the captions. Such figures present the contour plot of CWT absolute value as a function of the scale and translation parameters of wavelet.

Reviewer #2

1) The word "modeshapes" should be replaced by "mode shapes" throughout the article.
Done

2) In the sentence "the local stiffness kc due to the crack is evaluated … through the following polynomial expression" (at the end of page 4) the word "polynomial" should be deleted as the polynomial appears at the denominator in formula 4.
Done, thank you

3) Formula 4 should be corrected as at the numerator tb^2 should be bh^2
Done

4) Before formula (11) "…data, <eta>(x), is fitted…" should be "…data, <eta>(x), are fitted…"
Done

5) In formula (11.2) the expression 0 <x2 <-L(1-<beta>2) is wrong.
The expression has been amended

6) It is not clear if the origin of the x2-coordinate coincides with the right or with the left end of the beam. If it is the left end, in formula (12.2) the expression 0 <x2<<LAMBDA>s should be corrected.
The origin of the x2-axis is at the right of the beam, so Eq. 12.2 is correct.

7) For the sampling step defined after formula 12 it would be better to use the symbolism <DELTA>x instead of dx which is a differential.
Done

8) In the first line of section 4.3 "…… deflections of the beam …" should be "…… deflections of the cantilever beam …"
Done

9) The Section entitled "Summary of padding method comparison" should be 4.4 and not 4.3.
Done

10) The method proposed has been applied for a number of measuring points N = 1000. However, from an experimental point of view, even with a Scanning Laser Vibrometer, the number of measurements points is considerably lower and consequently the sensitivity of CWT will be influenced. Therefore it would be

interesting to plot diagrams comparing the results of the linear padding method, Messina's method and the proposed polynomial method such as those shown in figure 10 for N=1000, but with N=50/100 in order to represent a more realistic case.

The results being presented (e.g. see those in Fig. 10) for a sampling interval Δx = 0.001L, seem to be confirmed by taking a larger value such as Δx = 0.01L. However, when a larger value of sampling interval is considered, a smaller value of wavelet scale has to be chosen (see the new Ref. [29] in the revised version of the manuscript) in order to obtain the same damage identification capacity. A figure has been added in the revised version to show the trend of the minimum detectable crack size as a function of the signal-to-noise ration SNR for the 1st mode shape in a cantilever beam when Δx = 0.01L (sampling points equal to 100).

Highlights

- CWT edge effects in identifying damage close to beam ends is analysed
- New polynomial padding method, based on polynomial fitting functions, is proposed
- Noisy modeshapes and static deflections of cracked beams are simulated
- Proposed method is compared with literature padding methods

Revised version, June 2014

A PADDING METHOD TO REDUCE EDGE EFFECTS FOR ENHANCED DAMAGE IDENTIFICATION USING WAVELET ANALYSIS

Lorenzo MONTANARI[1,a], Biswajit BASU[2,b], Andrea SPAGNOLI[*1,c], Brian M. BRODERICK[2,d]

[1]Department of Civil-Environmental Engineering and Architecture, University of Parma
Parco Area delle Scienze 181/A, 43124 Parma, Italy

[2]Department of Civil, Structural and Environmental Engineering, Trinity College, Dublin 2, Ireland
[a]lollomonta@gmail.com, [b]basub@tcd.ie, [c]spagnoli@unipr.it, [d]bbrodrck@tcd.ie

ABSTRACT. Vibration response based structural damage identification by spatial wavelet analysis is widely considered a powerful tool in Structural Health Monitoring (SHM). This work deals with the issue of border distortions in wavelet transform that can mask tiny damages close to the boundary of a structure. Since traditional padding methods (e.g. zero-padding, symmetric padding, linear padding) are often not satisfactory, a simple and computationally inexpensive signal extension method, based on fitting polynomial functions and continuity conditions at the extrema, is proposed. The method is applied to analyze noisy ~~modeshape~~mode shapes and static deflection of cracked cantilever and simply supported beams. The effectiveness and the versatility of the method in localizing tiny damages close to clamped, free or hinged beam boundaries is demonstrated. Furthermore, an extensive comparison with the linear padding method and Messina's isomorphism methods is carried out.

KEYWORDS: border distortions; padding method; false indication; vibration-based damage identification; continuous wavelet transform; cracked beam.

1. INTRODUCTION

In several aerospace, civil and mechanical structures, during their service life damage can nucleate, accumulate and propagate leading to out-of-service conditions and, sometimes, dangerous

*Corresponding author: phone +39 0521905927, fax +39 0521905924

collapses. Therefore, Structural Health Monitoring (SHM) is an essential tool in identifying the presence and the evolution of possible damage. In the last few decades, researchers have put a great effort in developing different vibration response based damage identification methods [1,2] to replace traditional non-destructive techniques (e.g. acoustic, ultrasonic, magnetic field, radiograph, eddy-current, thermal field methods) [3], which exhibit the drawbacks of requiring a priori knowledge of damage location and its accessibility.

Among the recent vibration-based structural damage detection techniques, also called intelligent damage diagnosis methods [2], Wavelet Analysis (WA) has been widely recognized as an effective and robust damage detection tool due to its capability to deal with non-stationary signals and to localize singularities in a function or in any of its derivatives [4]. Liew and Wang [5] and Wang and Deng [6] first analysed the numerical and experimental structural responses of simple cracked beams by Wavelet Transform (WT) in the space domain to identify damage. They highlighted that wavelet analysis, due its multi-resolution properties, is capable of identifying a singularity in beam deflection due to damage at the crack location through a local jump or peak of the wavelet coefficients. Subsequently other authors (Pakrashi et al. [7], Gentile and Messina [8], Rucka and Wilde [9,10], Loutridis et al. [11], Wang and Wu [12]) examined in more depth the damage detection problem by WA by analyzing numerical and experimental, static and dynamic noisy responses of damaged or multi-damaged (cracked, delaminated, etc.) structural components through wavelet functions having different basis.

Despite the effectiveness of wavelet analysis in damage identification, a reliable detection of tiny damages is still an open challenge because they can be masked by measurement noise and/or edge (border) distortion of the wavelet transform. While the technology is progressing in the development of SHM techniques for spatially distributed measurements [7, 13-15] (e.g. networks of distributed sensors, optical fibers, computer vision and laser scanning techniques), the issue of edge effects in Continuous Wavelet Transforms (CWT) remains poorly addressed in the literature [9-10, 16-17].

It is well known that border effects are very common in many finite-length non-stationary signal analysis and processing approaches (e.g. WT, Hilbert-Huang transform) [4,18-19]. As near the signal ends, the convoluting window extends partially on the signal domain, abnormal coefficients arise and taint the transform. To handle boundary effects two type of approaches are usually used: the first is to impose some extra constraints on the signal (e.g. extension method) while the second is to construct a specific wavelet. For their simplicity the signal boundary constraint approaches are preferred. Traditional extending methods as zero padding, periodic padding, symmetric padding and linear padding (e.g. see MATLAB Wavelet Toolbox [20]), are usually employed in WA but often case-dependent models are needed to conveniently alleviate the border effects for the specific application. Kijewski and Kareem [21] and Su et al. [22] discussed extensively the edge effect problem in wavelet-based analysis employing the Morlet wavelet, suggesting, respectively, a simple extension method to preserve the local spectral content of the signal and a smooth extension scheme using a Fourier-based method to preserve the signal time-varying characteristics. Williams and Amaratunga [23] developed an extrapolated Discrete Wavelet Transform (DWT), applicable to Daubechies and biorthogonal wavelet bases, which does not exhibit edge effects in image compression and other signal processing applications. A non-linear extension model for CWT,

named the Leap-Step Time Series Analysis (LSTSA) model, was proposed by Zheng et al. [24] to enhance the detection of low-frequency signals in the observed Length-Of-Day (LOD) series.
As mentioned above, few researchers have examined in depth the problem of WT border distortion, despite its significant influence in masking damage. In fact, since the damage tends to nucleate and propagate in the most highly stressed zone of the structure, if this zone is near the boundary (e.g. the area close to the clamped section of a cantilever) than the maximum WT coefficients due to the edge effects will mask the damage, leading to situations of false indication or even of false alarm. Spanos et al. [16] considered multi-damaged Euler-Bernoulli beams subjected to static loads and numerically showed that applying the WT on the difference between the damaged and the undamaged beam responses, boundary effects are eliminated and damage-related to local maxima are clearly identified. Rucka and Wilde, imposing the local continuity of the first and second derivatives at the ends, extended the signal outside its original support through a simple cubic spline extrapolation based on three [9] or four [10] neighbouring points. On the other hand, Messina in [17] discusses extensively the border distortion in CWT dealing with the first four Gaussian wavelets and proposed two methods. The first method consists of padding the signal through isomorphisms (called "Rotation" – corresponding to a polar-like symmetry - and "Turnover" – corresponding to a mirror symmetry) of the original signal. The author examined their quality in limiting the border distortions with respect to the beam boundary conditions and the derivative order. The second method (called "Self-minimization") aims at correcting a first approximated extension (e.g. obtained by a fitting polynomial) by minimizing an objective function which depends on the convolution results.
In the present paper, the problem of the damage masked by CWT border distortions is discussed and a new signal extension polynomial method to enhance damage detection by spatial CWT is proposed. The method is based on high-order polynomial functions that fit the original data and its first derivative so as to extend smoothly the signal and its derivatives. To illustrate the effectiveness and the versatility of the method with respect to different boundary conditions and beam deflections (described by either trigonometric or polynomial functions), the free vibrations and the static deflection of a cracked cantilever, and the free vibrations of a cracked simple supported beam are numerically simulated. A synthetic Gaussian white noise is added to the signal to represent real measured data. The fourth order Coiflet basis function is used in wavelet analysis. The method is compared with the traditional linear padding method and with Messina's isomorphism methods.

2. MODELLING OF THE CRACKED BEAM

A cracked Euler-Bernoulli beam characterized by an open edge crack under different boundary conditions at the two ends, i.e. clamped-free (cantilever beam) and supported-supported (simply supported beam), is considered (Fig. 1). The free vibration response of both cantilever and simply supported beams as well as the static deflection of the cantilever beam due to the point load F are analytically evaluated solving the free vibration equations or the static equilibrium equations of the two uncracked sub-beams connected by a rotational spring (representing the local stiffness k_c of the cracked cross-section of the beam) at the crack location, x_c. The beam has a rectangular cross-section with height h and width b; the crack depth is a and L is the beam length. The symbols I, A, E

and ρ represent respectively, moment of inertia and area of the cross-section and Young modulus and density of the material.

Figure 1

2.1. Free vibration

The free vibration response of the two uncracked parts of the beam can be written as

$$EI\frac{\partial^4 v(x,t)}{\partial x^4}+\rho A\frac{\partial^2 v(x,t)}{\partial t^2}=0 \tag{1}$$

where $v(x, t)$ is the transversal displacement of the beam from its static equilibrium position at a distance x from the left end at the time t. Separating the variables in Eq. (1) ($v(x,t)=\eta(x)\,g(t)$) and solving the characteristic equation function of x, the ~~modeshape~~mode shapes η_L and η_R of the left and right sub-beam respectively, are as follows

$$\eta_L=C_{1L}\sin(\alpha x)+C_{2L}\cos(\alpha x)+C_{3L}\sinh(\alpha x)+C_{4L}\cosh(\alpha x)\quad 0\le x<x_c \tag{2.1}$$

and

$$\eta_R=C_{1R}\sin(\alpha x)+C_{2R}\cos(\alpha x)+C_{3R}\sinh(\alpha x)+C_{4R}\cosh(\alpha x)\quad x_c\le x\le L\,. \tag{2.2}$$

where $\alpha=\left(\frac{\rho A\omega^2}{EI}\right)^{1/4}$ and ω is the natural frequency of the cracked beam.

The $C_{(.)}$ terms are integration constants arising from the solution of a fourth order differential equation in space. By imposing the boundary conditions (Eqs. 3) a system of eight linear equations is formed. The natural frequencies of the cracked beam are found by setting the determinant of the matrix of the linear system to zero, and solving it numerically for the roots of α. The coefficient C_{1L} is imposed to be equal to unity.

The boundary conditions of the cantilever beam at the clamped and at the free end are, respectively:

$$\eta_L(0)=0 \quad\text{and}\quad \eta_L'(0)=0\,, \tag{3.1}$$

$$\eta_R''(L)=0 \quad\text{and}\quad \eta_R'''(L)=0\,. \tag{3.2}$$

While the boundary conditions of the simple supported beam at the two ends are:

$$\eta_L(0)=0 \quad\text{and}\quad \eta_L''(0)=0\,, \tag{3.3}$$

$$\eta_R(L)=0 \quad\text{and}\quad \eta_R''(L)=0\,. \tag{3.4}$$

For both the structures, the conditions of continuity of displacement, moment and shear at the crack location can be expressed as

$$\eta_L(x_c)=\eta_R(x_c)\,,\quad \eta_L''(x_c)=\eta_R''(x_c)\ \text{ and }\ \eta_L'''(x_c)=\eta_R'''(x_c)\,. \tag{3.5}$$

The rotational spring at the cracked section introduces a discontinuity of the rotation, which can be written as

$$\eta_R'(x_c)-\eta_L'(x_c)=\frac{EI}{k_c}\eta_R''(x_c)\,. \tag{3.6}$$

The local stiffness k_c due to the crack is evaluated, according to linear elastic fracture mechanics concepts, through the following ~~polynomial~~ expression [25]

$$k_c = \frac{bh^2 E}{24\left(\delta/(1-\delta)\right)^2 (5.93 - 19.69\delta + 37.14\delta^2 - 35.84\delta^3 + 13.12\delta^4)}. \quad (4)$$

where $\delta = a/h$ is the relative crack depth.

2.2. Static deflection

The static deflection of the cracked cantilever subjected to a concentrated force, *F*, at the free end (*x*=*L*), can be modeled starting from the second order static equilibrium equation of the sub-beams at the left and right sides of the cracked section

$$\frac{d^2\eta(x)}{dx^2} = \frac{M(x)}{EI}. \quad (5)$$

where *M*(*x*), the bending moment along the beam due to the force *F*, is equal to $F(L-x)$. Imposing the boundary conditions described in Eqs. (3.1, 3.2, 3.5 and 3.6), the analytical solution of the problem becomes

$$\eta(x) = \frac{F}{EI}\left(\frac{Lx^2}{2} - \frac{x^3}{6}\right) \quad 0 \le x < x_c \quad (6.1)$$

and

$$\eta(x) = \frac{F}{EI}\left(\frac{Lx^2}{2} - \frac{x^3}{6}\right) + \frac{F(L-x_c)}{k_c}(x - x_c) \quad x_c \le x \le L \quad (6.2)$$

3. DAMAGE DETECTION BY SPATIAL CWT

3.1. Wavelet analysis

Thanks to its multi-resolution properties, wavelet analysis, acting as a signal microscope, has the ability to analyze non-stationary signals in more detail than traditional analysis tools, such as Fourier transform or Short-Time Fourier transform.

A wavelet function $\psi(x)$ is a zero mean local wave-like function which decays rapidly, and which satisfies particular conditions [4]. A family of wavelet functions may be obtained by considering:

$$\psi_{k,s}(x) = \frac{1}{\sqrt{s}}\psi\left(\frac{x-k}{s}\right), \quad (7)$$

where *s* and *k* are, respectively, the scale and the translation parameters. The continuous wavelet transform of a signal $\eta(x)$ with respect to the wavelet function $\psi(x)$ is defined as

$$W(k,s) = \int_{-\infty}^{+\infty} \eta(x)\frac{1}{\sqrt{s}}\psi^*\left(\frac{x-k}{s}\right)dx \quad (8)$$

where ψ^* is the complex conjugate of ψ.

Since the identification of a discontinuity in a function or in any of its derivatives can be linked to the number of vanishing moments of the analyzing wavelet function [7], it is possible for a wavelet transform to detect singularities in a signal or its derivatives by choosing an appropriate basis

function $\psi(x)$. Since the presence of an open crack in a beam may introduce a singularity in the derivatives of the deflected shape, wavelet transforms are considered to be a powerful tool to locate the damage. Due to the presence of the singularity, a transformed deflected shape yields a local variation or extremum in the wavelet coefficient at the location of damage throughout the different scales. Wavelet functions with a high number of vanishing moments are appropriate for damage identification purposes, such as the 4^{th} order Coiflets ('Coif4') and the 8^{th} order Symlets ('Sym8'), which both have 8 vanishing moments. Following the suggestion of Pakrashi et al. [7], the 'Coif4' basis function is used throughout the present work. A MATLAB routine to perform the CWT with 'Coif4' has been implemented by the authors to improve the accuracy of the existing MATLAB procedure (the built-in routine approximates the signal thorough a constant piecewise function, while that implemented in this study considers a piecewise linear trend).

3.2. Edge effects and signal extension

As mentioned above, the continuous wavelet transform is defined by the convolution of the input signal, $\eta(x)$, with a wavelet function generated from the mother wavelet, $\psi(x)$, by scaling and translating it. For a finite-length signal, when the convolution operation is executed close to the signal ends, the wavelet window extents into a region with no available data, so that the transform values close to the borders of the signal are tainted by the non-existing data. Consequently, the values of the CWT coefficients very close to the signal extrema arise abnormally (border distortions) and the real signal features of that region are consequently corrupted by the transform. So edge effects can provoke the masking of the damage and yield false indicators (see Section 4).
Among the different approaches to handle edge effects, the most commonly used one is to preprocess the signal through extrema extension [4,18]. Traditional extension techniques include extension by zero padding, periodicity, symmetry and linearization [20]. These methods make simple assumptions about the signal characteristics outside the borders but they prove unsatisfactory for many applications [21-24], including damage detection [9-10,17].
According to the cracked beam model of Section 2, a damage introduces a discontinuity (jump) in the rotation, $\eta'(x)$, of the structural response and consequently a singularity in the curvature, $\eta''(x)$, and in the subsequent derivatives. As is well-known [7], a wavelet with m vanishing moments detects the local discontinuities of the signal and of its derivatives up to the mth order. Therefore, padding functions to be added at either end of the original signal, need to have specific smoothness features to avoid introducing edge discontinuities into the padded signal or its derivatives up to the mth order. The traditional padding methods cited above introduce discontinuities at the ends of the signal and/or in its 1st or 2nd derivatives, so that small damages close to the beam extrema are masked by CWT border distortions. Hence, an ad-hoc extension method that minimizes edge effects must be employed for effective damage detection through wavelet analysis.

3.3. The proposed padding method

Realistic situations where noise is superimposed on the original signal are considered in the following. As a matter of fact, the ideal situation in the absence of noise has a trivial solution as by extending the signal, $\eta(x)$, through its interpolating spline, the border distortions are suppressed and the location of very tiny damages close to the edges are always identified by WT. It is also noted that in the absence of noise WA is not necessary to detect the damage position since by numerically calculating the second derivative of the original signal, the damage location can be readily identified [26]).

The presence of noise is introduced by adding a synthetic Gaussian white noise to the original response. To quantify the noise level, the signal to noise ratio (SNR) is considered. The SNR, expressed in decibels, is defined as

$$SNR = 10\log_{10}\left(\frac{P_{signal}}{P_{noise}}\right). \tag{9}$$

The term P with the subscripts in Eq. (9) denotes power and is computed as

$$P_{(.)} = \frac{1}{N_z}\sum_{i=0}^{N_z-1}|z(x_i)|^2, \tag{10}$$

where N_z denotes the number of discrete points of a generic sampled function $z(x)$. Note that different measurements of the noise can be adopted. For instance by considering a signal-to-noise ratio SNR* defined as $10\log_{10}\left(\max_{signal}/\sigma_{noise}\right)$ ($\max_{signal}$ = maximum absolute value of the signal, σ_{noise} = standard deviation of the signal), we have: SNR=120dB corresponds to about SNR*=63dB, SNR=100dB corresponds to about SNR*=53dB and so on.

It can be shown, through numerical experiments, that approaches to extend the noisy signal either through its interpolating spline or its fitting spline (as suggested in [9-10]) prove not to be effective. Therefore, a simple and computationally efficient method based on using two polynomial functions $f_1(x_1)$ and $f_2(x_2)$ to extend, in the range $x \le 0$ and $x \ge L$, respectively, the signal $\eta(x)$ is proposed (Fig. 2). These functions are obtained by a fitting procedure in order to:

(i) describe correctly $\eta(x)$ in such a way to extend smoothly the trend of the signal and of its derivatives up to the order equal to the *m*th vanishing moment of the adopted wavelet;

(ii) ensure continuity at the boundaries up to *m*th derivative order.

Since the original signal is corrupted by noise, conditions (i) and (ii) may only be satisfied in an average sense.

When adopting the 'Coif4' wavelet with 8 vanishing moments, boundary continuities up to the 8th derivative of $\eta(x)$ have to be satisfied. Hence, polynomial functions of degree 8 are generated for $f_1(x_1)$ and $f_2(x_2)$.

To define the extension functions, firstly the original noisy data, $\eta(x)$, ~~is~~ are fitted in a least squares sense through two polynomial functions $\bar{f}_1(x_1)$ and $\bar{f}_2(x_2)$ as

$$\bar{f}_1(x_1) = \bar{A}_1x_1^8 + \bar{B}_1x_1^7 + \bar{C}_1x_1^6 + \bar{D}_1x_1^5 + \bar{E}_1x_1^4 + \bar{F}_1x_1^3 + \bar{G}_1x_1^2 + \bar{H}_1x_1 + \bar{I}_1 \quad \text{with} \quad 0 \le x_1 \le \beta_1 L \tag{11.1}$$

and

$$\bar{f}_2(x_2) = \bar{A}_2x_2^8 + \bar{B}_2x_2^7 + \bar{C}_2x_2^6 + \bar{D}_2x_2^5 + \bar{E}_2x_2^4 + \bar{F}_2x_2^3 + \bar{G}_2x_2^2 + \bar{H}_2x_2 + \bar{I}_2 \text{ with} \tag{11.2}$$

~~$0 \le x_2 \le L(1-\beta_2)$~~ $-L(1-\beta_2) \le x_2 \le 0$,

where $\bar{A}_1, \bar{B}_1, \ldots, \bar{I}_1$ and $\bar{A}_2, \bar{B}_2, \ldots, \bar{I}_2$ are the coefficients of the fitting polynomial functions, $\bar{f}_1(x_1)$ and $\bar{f}_2(x_2)$, respectively. The function $\bar{f}_1(x_1)$ fits $\eta(x)$ from $x = 0$ to $x = \beta_1 L$; while $\bar{f}_2(x_2)$ fits $\eta(x)$ from $x = L(1-\beta_2)$ to $x = L$, where β_1 and β_2 can vary in the range $0.1-1$. There are not optimal values for these parameters, as they depend on the trend of the signal and the noise level. For instance in the case of signals characterized by no sign change of first derivative, values in the range of $0.7-1$ work well while for oscillating signals values in the range $0.1-0.4$ are suggested; moreover the latter values are preferred in the presence of low noise content (see Section 4).

The extension polynomials $f_1(x_1)$ and $f_2(x_2)$, having the same degree of the fitting functions, are

$$f_1(x_1) = A_1 x_1^8 + B_1 x_1^7 + C_1 x_1^6 + D_1 x_1^5 + E_1 x_1^4 + F_1 x_1^3 + G_1 x_1^2 + H_1 x_1 + I_1 \quad \text{with} \quad -\Lambda s \le x_1 \le 0 \tag{12.1}$$

and

$$f_2(x_2) = A_2 x_2^8 + B_2 x_2^7 + C_2 x_2^6 + D_2 x_2^5 + E_2 x_2^4 + F_2 x_2^3 + G_2 x_2^2 + H_2 x_2 + I_2 \text{ with } 0 \le x_2 \le \Lambda s \tag{12.2}$$

where s is the scale parameter considered in the WA, Λ represents the distance from the mother wavelet center to the position where the wavelet attains negligible values (for 'Coif4', $\Lambda = 11dx$ is assumed, where ~~d~~Δx is the sampling step), and $A_1, B_1, \ldots, I_1$ and $A_2, B_2, \ldots, I_2$ are the polynomial coefficients obtained as follows:

$$A_1 = \bar{A}_1;\ B_1 = \bar{B}_1;\ C_1 = \bar{C}_1;\ D_1 = \bar{D}_1;\ E_1 = \bar{E}_1;\ F_1 = \bar{F}_1;\ G_1 = \bar{G}_1;\ H_1 = \bar{H}_1;\ I_1 = \eta(x=0) \tag{13.1}$$

$$A_2 = \bar{A}_2;\ B_2 = \bar{B}_2;\ C_2 = \bar{C}_2;\ D_2 = \bar{D}_2;\ E_2 = \bar{E}_2;\ F_2 = \bar{F}_2;\ G_2 = \bar{G}_2;\ H_2 = \bar{H}_2;\ I_2 = \eta(x=L) \tag{13.2}$$

Then, the coefficients H_1 and H_2 are optimized against the first derivative $\gamma(x)$ of the padded noisy data, $f_1(x) \cup \eta(x) \cup f_2(x)$, numerically calculated at $x = 0$ and $x = L$ through Richardson's extrapolation [27], which allows a high-order approximation (e.g. $O(dx^8)$, $O(dx^{10})$ or $O(dx^{12})$) of the derivative. An iterative procedure is required since H_1 and H_2 are equal to $\gamma(x=0)$ and $\gamma(x=L)$, respectively, which in turn are functions of H_1 and H_2.

Since differentiating the original signal increases the amount of noise, the above described optimization approach is not effective for the other polynomial coefficients, $A_1, \ldots, G_1$ and $A_2, \ldots, G_2$. Note that the last two equalities of Eqs (13.1) and (13.2) impose the fundamental condition of signal continuity at the two extrema. Furthermore, it has to be underlined that good results can be achieved without performing the optimization procedure related to the first derivative (i.e. by assuming $H_1 = \bar{H}_1$ and $H_2 = \bar{H}_2$) and, in fact, better results could be obtained in some cases, e.g., when the noise level is high. Figures 2-4 show a generic noisy data signal, extended through the proposed polynomial functions $f_1(x_1)$ and $f_2(x_2)$, and its 1st and 2nd derivatives. These figures point out that the conditions (i) and (ii), explained above, are satisfied by the proposed method.

Figure 2

Figure 3

Figure 4

4. ILLUSTRATIVE EXAMPLES

The effectiveness and the versatility of the proposed polynomial padding method in minimizing the CWT border distortions is analyzed by considering the ~~modeshape~~mode shapes and the static deflection of both cantilever and simply supported cracked beams. Since the static deflection of a simply supported beam with a crack close to a support under a mid-span vertical point force coincides with that of a cantilever with a crack close to the free end, only the latter case is analysed in the following.

The method is assessed by considering analytical structural responses having different features (trigonometric function for the ~~modeshape~~mode shapes and cubic polynomial for the static responses) and constraint conditions (clamped, simple supported and free). The results are compared to those obtained by the traditional linear padding method [20] and Messina's isomorphism methods [17], experimented by the present authors to be the most effective padding method available in the literature. Note that the latter methods are chosen instead of the Messina's self-minimization method, as they are found to be comparatively more robust and effective (incidentally, in the conclusions reported in Ref. [17] Messina himself recommends to adopt isomorphism methods).

A cracked beam of length L = 1m and a rectangular cross-section of height $h = 0.05L$ and width $b = 0.5h$, constituted by an elastic linear isotropic material with Young modulus, E = 200 GPa, and density, ρ = 7850 kg/m^3, is considered.

The free vibration responses and the static deflections of the beams, sampled at ~~d~~$\Delta x = 0.001L$ intervals, are determined according to the model of Section 2. Such signals are analyzed through CWT, fixing the relative crack depth, δ, unless otherwise specified, to 2% and varying the crack locations, x_c, and the noise level (synthetic Gaussian white noise is used). The wavelet analyses are executed using the 'Coif4' mother wavelet.

4.1 Free vibration response of a cantilever beam

The normalized first ~~modeshape~~mode shape (maximum deflection equal to unity) of the damaged cantilever beam is analysed using the linear padding method, Messina's method (with the "Turnover" method at the clamped end and the "Rotation" method at the free end [28]) and the proposed method (with the fitting parameters, β_1 and β_2 assumed equal to 1). The crack is located at $x = 0.02L$ from the clamped end. A noise level SNR = 120 dB is assumed.

In Fig. 5a, where the linear padding method is used, a jump in the curvature is evident at $x = 0$. In Fig. 5b, where the "Turnover" method is applied to the clamped end, the continuity of the second derivative at $x = 0$ is fulfilled while a jump of the third derivative is expected. On the other hand, in Fig. 5c, thanks to the proposed polynomial padding, no discontinuities are present in the boundaries and the extending functions are in agreement with the average trend in the curvature $\eta''(x)$. It is worth noticing that, for the selected combination of noise level and damage severity and location, it is not possible to locate the crack by analyzing the curvature plot, and hence a wavelet transform technique is necessary to detect such damage.

Figure 5

Figures 5d-f present zooms on the contour plots of the absolute values of the CWT (from scale 1 to scale 40) of the normalized first ~~modeshape~~mode shape padded using the three methods presented above. In the contour plots, the lighter colors represent high coefficient values, whilst darker colors correspond to low coefficient values (see the color bar on the right of Figs. 5d-f). Since a wavelet with more than one vanishing moment (in our case 'Coif4') associates high coefficient values to the signal discontinuities and since high wavelet scales are able to detect a discontinuity even if the wavelet is not centered on it, the contour plot displays a shape pattern characterized by a central bright cone and a number of adjacent less bright cones, all pointing towards the singularity region.
Since the linear padding method introduces a discontinuity in the second derivative at $x = 0$ (Fig. 5a), high coefficient values arise around that region and the bright cone points towards $x = 0$ (Fig. 5d). The damage location is consequently masked because of the edge effects. Furthermore if only the CWT coefficients related to a given scale were considered (e.g. scale 24 in Fig. 6a), the analysis would locate erroneously the damage at about $x = 0.01L$.
When Messina's method is applied, even if a jump in the third derivative occurs at $x = 0$, crack discontinuity at finer and medium scales can be detected as the contour cones point correctly towards the crack location at $x = 0.02L$ (Fig. 5e). On the other hand, at coarser scales, characterized by narrower bands of lower frequencies, the CWT detects the jump of the third derivative and hence it is unable to locate the damage.
Figure 5f shows that, when the proposed polynomial extension method is used, the central bright cone is characterized by an axis centered to the correct damage location. Therefore crack position can be detected at all CWT scales, leading to unambiguous and more reliable damage identification.

The contour plots of the absolute values of the CWT of the normalized third ~~modeshape~~mode shape of the cracked cantilever beam obtained using Messina's method and the proposed polynomial method are presented in Fig. 6 (the crack is located close to the free end at $x = 0.98L$ and a noise level SNR = 140 dB is imposed). Given the oscillating feature of the ~~modeshape~~mode shape, β_1 and β_2 are assumed equal to 0.2 and 0.333, respectively.
Figures 6a and 6b demonstrate that wavelet analysis fails to detect the damage near the free end when Messina's method is applied. This is a consequence of the fact that the curvature near the free end tends to be null and therefore damage identification is more difficult. The jump in the ~~modeshape~~mode shape third derivative at $x = 0$ due to the use of the "Turnover" padding method is the main discontinuity that 'Coif4' wavelet detects in analyzing the padded signal.
On the other hand, using the proposed polynomial padding method, no discontinuity is present at the extrema of the signal or its derivatives, and no border distortion is generated by the wavelet transform. The bright cones point properly to the damage position (see Figs 6c-d).

Figure 6

4.2 Free vibration response of a simply supported beam

Figure 7 shows the effectiveness of Messina's method (the "Rotation" method is applied at both extrema) and the proposed polynomial method (β_1 and β_2 are equal to 1) in the case of the first ~~modeshape~~mode shape of a cracked simply supported beam corrupted by noise (SNR = 140 dB). The crack, close to the left support at $x = 0.02L$, is correctly identified through both methods. Note that when applied to zero curvature ends, Messina's method does not introduce a discontinuity in the signal or its derivatives, and hence no border distortion occurs. Note also that the brightest cone of Fig. 7a is shifted at coarser scales to the left with respect to the damage location due to the presence of the mirrored damage at $x = -x_c$.

Figure 7

4.3 Static deflection

The normalized noisy static deflections of the cantilever beam subjected to the point load F of Fig. 1, with an open crack of relative depth $\delta = 2\%$, located at $0.02L$ or at $0.098L$, are analysed by CWT. The polynomial extension method is applied assuming β_1 and β_2 equal to 1 and compared with Messina's method. It is observed that even if $\eta(x)$ is a cubic function and the continuity of $\eta(x)$ and its derivatives at the boundaries can be satisfied by polynomial functions of degree three, the presence of noise requires extending polynomial functions in general of eighth order to overcome edge effects.

Both methods prove to be effective in analyzing static deflection when the crack is close to the clamped end (Fig. 8) or when it is near the free end (Fig. 9).

Considering a noise level of SNR = 100 dB, since finer scales are more sensible to noise than coarser ones, the lower parts (from scale 1 to 20) of the CWT contour plots in Figs. 8a and 8c provide somewhat ambiguous damage detection for both considered methods. On the other hand, by considering the upper parts of these contour plots, (from scale 20 to 40), the damage location can clearly be identified (Figs. 8b and 8d).

Figure 8

Fig. 9 compares the effectiveness of the two methods in removing edge effects as the noise level increases. When noise level is at SNR = 100 dB, the damage is clearly located by both methods. Increasing the noise level to SNR = 90 dB the damage is partially masked, while at SNR = 80 dB, the noise completely masks the damage. This behavioral trend demonstrates that CWT border distortions are effectively suppressed by both methods, but damage is masked when a certain level of noise (which is dependent on the specific beam features and damage location and severity) is present.

Figure 9

4.43 Summary of padding method comparison

The linear padding method, Messina's isomorphism methods and the proposed polynomial extension method are qualitatively compared in Figure 10 for a range of ~~modeshape~~mode shapes and static deflections obtained by varying the crack depth ($\delta = 0.0001 - 0.9$) and its location (x = $0.02L$ or x = $0.98L$) (see Fig. 10). Crack depth is incremented by $d\delta = 10^{-j-2}$ throughout the range $10^{-j-1} < \delta \le 10^{-j}$ where $j = 0,1,2,3$. For a given noise level, the identification criterion considers that the damage is correctly detected if the highest absolute value of the CWT at the scale 24 falls exactly at the crack location with each of 25 different noise random distributions. Figure 10 identifies the minimum crack depth sizes correctly identified by each method with a given SNR. In these analyses, the fitting parameters β_1 and β_2 equal 1, except in the analysis of the second ~~modeshape~~mode shape of the cantilever beam, where $\beta_1 = 0.15$ and $\beta_2 = 0.125$, and the first ~~modeshape~~mode shape of the simply supported beam, where $\beta_1 = \beta_2 = 0.1667$. Moreover for the second ~~modeshape~~mode shape of the cantilever beam, the values $H_1 = \overline{H}_1$ and $H_2 = \overline{H}_2$ are employed as coefficients of the extension polynomial function.

Figure 10 clearly shows, for all the conditions analysed, the weakness of the linear padding method in tackling border distortions. For instance, when the first ~~modeshape~~mode shape of the cantilever beam with x_c = $0.98L$ is analysed, even cracks of about $\delta = 0.9$ are masked by edge effects. Moreover, at a given noise level, the minimum crack size that can be identified using the linear padding method is larger than those that can be detected using the other methods. For both the linear padding method and Messina's method, the plots in Figure 10 display plateau representing the minimum crack size that can be correctly detected irrespective of SNR. In the linear padding method this plateau occurs because 'Coif4' recognizes the dominance of the discontinuity in the second derivative at x = 0 over the discontinuity introduced to the first derivative by the crack. The crack size identified by the plateau is the smallest that can be identified in this particular structure. As expected, at higher noise levels, the minimum damage that can be detected increases.

With Messina's method, the observed plateaus in the δ-SNR curves are attributable to the discontinuity in the third derivative at x = 0 related to the "Turnover" method. Since a jump in the third derivative has less influence on the CWT than one in the second derivative, the smallest crack detectable using Messina's method at a given SNR is smaller than that detectable using the linear padding method. When Messina's method is applied to the ~~modeshape~~mode shapes of the simply supported beam, the minimum identified δ decreases monotonically with increasing SNR (Fig. 10d). As mentioned above, this is due to the fact that the "Rotation" method applied to zero curvature ends does not yield edge discontinuities in all the signal derivatives. With damage at x = $0.98L$ in a cantilever beam, Messina's method is much more effective when applied to the static deflection than to the first ~~modeshape~~mode shape (see Figs. 10f and 10c). This arises because the first to the mth derivatives of ~~modeshape~~mode shape are all non-zero whilst the derivatives of the cubic static deflection are null from the 4th. As 'Coif4' analyses high order derivatives, the weight of the jump in the third derivative at x = 0 is more substantial in the ~~modeshape~~mode shape.

The proposed polynomial padding method is observed to be the most effective and versatile method in analyzing different structural responses corrupted by different noise amounts. At severe noise

levels, the proposed polynomial method and Messina's method succeed in identifying very similar minimum damage levels. However, at medium-to-low noise levels, the polynomial method is more successful in removing CWT border distortions, and is capable of identifying smaller cracks than either of the other methods.

Figure 10

The results being presented in Fig. 10 for a sampling interval $\Delta x = 0.001L$ seem to be confirmed by taking a larger value of the sampling interval. For instance, the same damage identification capacity obtained in the above with $\Delta x = 0.001L$ can be attained by considering a larger sampling interval, provided that a smaller wavelet scale is chosen (the need for a smaller wavelet scale as the sampling interval gets larger is discussed in Ref. [29]). Figure 11 presents the minimum detectable crack size as a function of the signal-to-noise ratio SNR for the first mode shape, sampled at $\Delta x = 0.01L$, in a cantilever beam with crack at $x_c = 0.02L$. The trends turn out to be similar to those reported in Fig. 10a for $\Delta x = 0.001L$.

Figure 11

5. CONCLUSIONS

When wavelet analysis is employed in vibration-based structural damage identification, the issue of border distortions is often crucial as it tends to mask damage near the edges of the structure where high stress levels are liable to occur. Since traditional padding methods are not satisfactory when small near-edge damages need to be detected, an effective and computationally efficient signal extension method is proposed to enhance damage detection by CWT. The method is based on the approach of padding the original signal using two functions that satisfy continuity conditions and extend the average trend and derivatives of the noisy signal. The two high degree polynomial functions employed are determined by imposing signal and first derivative extrema continuity conditions.

To investigate the effectiveness and the versatility of the proposed padding method, the analytical free vibration and static deflection responses of cantilever and simply supported cracked beams were analysed. Variations in crack depth ratio and position are considered, and synthetic Gaussian white noise is introduced to the signal to emulate real measured data. CWT, applying the linear padding method, Messina's isomorphism methods and the proposed polynomial method, is executed to detect the position of damage in the different structural configurations at different noise levels.

The CWT contour plots in the scale from 1 to 40 are analysed. While the linear padding method is generally poor, failing to identify small- and even medium-sized damage close to the beam ends, Messina's method works much better when the crack is close to the cantilever fixed end or when the sinusoidal free vibration of the simply supported beam is analysed. When applied to cantilever beam ~~modeshape~~mode shapes Messina's method does not perform as well. The proposed

polynomial method proved to be the most powerful method in dealing with the full range of structural configurations and damage considered. In particular, smaller cracks can be identified using the proposed method than with either of the other methods, whose formulations introduce a minimum bound on the crack size that can be correctly detected.

In summary, while damage identification using wavelet-based techniques is still an open challenge in the presence of high noise levels, the proposed signal extension method supports improved detection of small damage near beam edges through the minimization of wavelet transform border distortions.

REFERENCES

[1] H. Sohn, C.R. Farrar, F.M. Hemez, D.D. Shunk, D.W. Stinemates, B.R. Nadler, J.J. Czarnecki, A review of structural health monitoring literature: 1996-2001, Los Alamos National Laboratory, LA-13976-MS, 2004.

[2] Y.J. Yana, L. Cheng, Z.Y. Wua, L.H. Yam, Development in vibration-based structural damage detection technique, Mechanical Systems and Signal Processing 21 (2007) 2198-2211.

[3] J.E. Doherty, Nondestructive Evaluation, in: A.S. Kobayashi (Edt.), Handbook on Experimental Mechanics, Society for Experimental Mechanics Inc, 1987.

[4] S. Mallat, A wavelet tour on signal processing, third ed., Academic Press, New York, 2008.

[5] K.M. Liew, Q. Wang, Application of wavelet theory for crack identification in structures, Journal of Engineering Mechanics 124 (1998) 152-157.

[6] Q. Wang, X. Deng, Damage detection with spatial wavelets, International Journal of Solids and Structures 36 (1999) 3443-3468.

[7] V. Pakrashi, B. Basu, A. O'Connor, Structural damage detection and calibration using a wavelet-kurtosis technique, Engineering Structures 29 (2007) 2097-2108.

[8] A. Gentile, A. Messina, On the continuous wavelet transforms applied to discrete vibrational data for detecting open cracks in damaged beams, International Journal of Solids and Structures 40 (2003) 295-315.

[9] M. Rucka, K. Wilde, Crack identification using wavelets on experimental static deflection profiles, Engineering Structures 28 (2006) 279-88.

[10] M. Rucka, K. Wilde, Application of continuous wavelet transform in vibration based damage detection method for beams and plates, Journal of Sound and Vibration 297 (2006) 536-550.

[11] S. Loutridis, E. Douka, A. Trochidis, Crack identification in double cracked beams using wavelet analysis, Journal of Sound and Vibration 277 (2004) 1025-1039.

[12] Q. Wang, N. Wu, Detecting the delamination location of a beam with a wavelet transform: an experimental study, Smart Material and Structures 20 (2011) 012002.

[13] P.K. Rastogi, Optical Measurement Techniques and Applications, Artech House Inc, Boston, 1997.

[14] B. Trentadue, A. Messina, N.I. Giannoccaro, Detecting damage through the processing of dynamic shapes measured by a PSD-triangular laser sensor, International Journal of Solids and Structures 44 (2007) 5554-5575.

[15] J.M. Henault, M. Quiertant, S. Delepine-Lesoille, J. Salin, G. Moreau, F. Taillade, K. Benzarti. Quantitative strain measurement and crack detection in RC structures using a truly distributed fiber optic sensing system, Construction and Building Materials 37 (2012) 916-923.

[16] P.D. Spanos, G. Failla, A. Santini, M. Pappatico, Damage detection in Euler-Bernoulli beams via spatial wavelet analysis, Structural Control and Health Monitoring 13 (2006) 472-487.

[17] A. Messina, Refinements of damage detection methods based on wavelet analysis of dynamical shapes, International Journal of Solids and Structures 45 (2008) 4068-4097.

[18] A. Mertins, Signal Analysis: Wavelet, Filter Banks, Time-Frequency, Transforms and Applications, Wiley, Chichester, 1999.

[19] Y. Deng, W. Wang, C. Qian, Z. Wang, D. Dai, Boundary-processing-technique in EMD method and Hilbert transform, Chinese Science Bulletin 46 (11) (2001) 954-960.

[20] M. Misiti, Y. Misiti, G. Oppenheim, J. Poggi, Wavelet Toolbox, The MathWorks Inc, 2000.

[21] T. Kijewski, A. Kareem, On the presence of end effects and their melioration in wavelet-based analysis, Journal of Sound and Vibration 256 (5) (2002) 980-988.

[22] H. Su, Q. Liu, J. Li, Alleviating Border Effects in Wavelet Transform for Nonlinear Time-varying Signal Analysis, Advances in Electrical and Computer Engineering 11 (3) (2011) 55-60.

[23] J.R. Williams, K. Amaratunga, A Discrete Wavelet Transform Without Edge Effects Using Wavelet Extrapolation, Journal of Fourier Analysis and Applications 3 (4) (1997) 435-449.

[24] D. Zheng, B.F. Chao, Y. Zhou, N. Yu, Improvement of edge effect of the wavelet time-frequency spectrum: application to the length-of-day series, Journal of Geodesy 74 (2000) 249-254.

[25] H. Tada, P.C. Paris, G.R. Irwin, The Stress Analysis of Crack Handbook, second ed., Paris Production, St. Louis, 1985.

[26] A.K. Pandey, M. Biswas, M.M. Samman, Damage detection from changes in curvature mode shapes, Journal of Sound and Vibration 145(2) (1991) 321-332.

[27] K. Atkinson, An introduction to numerical analysis, Second ed., John Wiley & Sons, New York, 1989.

[28] N.I. Giannoccaro, A. Messina, G. Rollo, A damage detection based o the processing of multiple dynamic shapes through CWTs, Proceedings of The Sixth International Conference on Condition Monitoring and Machinery Failure Prevention Technologies, Dublin, 2009.

~~[28]~~[29] L. Montanari, Vibration-based damage identification in beam structures through wavelet analysis, PhD Thesis, Univerity of Parma, 2014.

Revised version, June 2014

A PADDING METHOD TO REDUCE EDGE EFFECTS FOR ENHANCED DAMAGE IDENTIFICATION USING WAVELET ANALYSIS

Lorenzo MONTANARI[1,a], Biswajit BASU[2,b], Andrea SPAGNOLI[*1,c], Brian M. BRODERICK[2,d]

[1]Department of Civil-Environmental Engineering and Architecture, University of Parma
Parco Area delle Scienze 181/A, 43124 Parma, Italy

[2]Department of Civil, Structural and Environmental Engineering, Trinity College, Dublin 2, Ireland
[a]lollomonta@gmail.com, [b]basub@tcd.ie, [c]spagnoli@unipr.it, [d]bbrodrck@tcd.ie

ABSTRACT. Vibration response based structural damage identification by spatial wavelet analysis is widely considered a powerful tool in Structural Health Monitoring (SHM). This work deals with the issue of border distortions in wavelet transform that can mask tiny damages close to the boundary of a structure. Since traditional padding methods (e.g. zero-padding, symmetric padding, linear padding) are often not satisfactory, a simple and computationally inexpensive signal extension method, based on fitting polynomial functions and continuity conditions at the extrema, is proposed. The method is applied to analyze noisy mode shapes and static deflection of cracked cantilever and simply supported beams. The effectiveness and the versatility of the method in localizing tiny damages close to clamped, free or hinged beam boundaries is demonstrated. Furthermore, an extensive comparison with the linear padding method and Messina's isomorphism methods is carried out.

KEYWORDS: border distortions; padding method; false indication; vibration-based damage identification; continuous wavelet transform; cracked beam.

1. INTRODUCTION

In several aerospace, civil and mechanical structures, during their service life damage can nucleate, accumulate and propagate leading to out-of-service conditions and, sometimes, dangerous

*Corresponding author: phone +39 0521905927, fax +39 0521905924

collapses. Therefore, Structural Health Monitoring (SHM) is an essential tool in identifying the presence and the evolution of possible damage. In the last few decades, researchers have put a great effort in developing different vibration response based damage identification methods [1,2] to replace traditional non-destructive techniques (e.g. acoustic, ultrasonic, magnetic field, radiograph, eddy-current, thermal field methods) [3], which exhibit the drawbacks of requiring a priori knowledge of damage location and its accessibility.

Among the recent vibration-based structural damage detection techniques, also called intelligent damage diagnosis methods [2], Wavelet Analysis (WA) has been widely recognized as an effective and robust damage detection tool due to its capability to deal with non-stationary signals and to localize singularities in a function or in any of its derivatives [4]. Liew and Wang [5] and Wang and Deng [6] first analysed the numerical and experimental structural responses of simple cracked beams by Wavelet Transform (WT) in the space domain to identify damage. They highlighted that wavelet analysis, due its multi-resolution properties, is capable of identifying a singularity in beam deflection due to damage at the crack location through a local jump or peak of the wavelet coefficients. Subsequently other authors (Pakrashi et al. [7], Gentile and Messina [8], Rucka and Wilde [9,10], Loutridis et al. [11], Wang and Wu [12]) examined in more depth the damage detection problem by WA by analyzing numerical and experimental, static and dynamic noisy responses of damaged or multi-damaged (cracked, delaminated, etc.) structural components through wavelet functions having different basis.

Despite the effectiveness of wavelet analysis in damage identification, a reliable detection of tiny damages is still an open challenge because they can be masked by measurement noise and/or edge (border) distortion of the wavelet transform. While the technology is progressing in the development of SHM techniques for spatially distributed measurements [7, 13-15] (e.g. networks of distributed sensors, optical fibers, computer vision and laser scanning techniques), the issue of edge effects in Continuous Wavelet Transforms (CWT) remains poorly addressed in the literature [9-10, 16-17].

It is well known that border effects are very common in many finite-length non-stationary signal analysis and processing approaches (e.g. WT, Hilbert-Huang transform) [4,18-19]. As near the signal ends, the convoluting window extends partially on the signal domain, abnormal coefficients arise and taint the transform. To handle boundary effects two type of approaches are usually used: the first is to impose some extra constraints on the signal (e.g. extension method) while the second is to construct a specific wavelet. For their simplicity the signal boundary constraint approaches are preferred. Traditional extending methods as zero padding, periodic padding, symmetric padding and linear padding (e.g. see MATLAB Wavelet Toolbox [20]), are usually employed in WA but often case-dependent models are needed to conveniently alleviate the border effects for the specific application. Kijewski and Kareem [21] and Su et al. [22] discussed extensively the edge effect problem in wavelet-based analysis employing the Morlet wavelet, suggesting, respectively, a simple extension method to preserve the local spectral content of the signal and a smooth extension scheme using a Fourier-based method to preserve the signal time-varying characteristics. Williams and Amaratunga [23] developed an extrapolated Discrete Wavelet Transform (DWT), applicable to Daubechies and biorthogonal wavelet bases, which does not exhibit edge effects in image compression and other signal processing applications. A non-linear extension model for CWT,

named the Leap-Step Time Series Analysis (LSTSA) model, was proposed by Zheng et al. [24] to enhance the detection of low-frequency signals in the observed Length-Of-Day (LOD) series.
As mentioned above, few researchers have examined in depth the problem of WT border distortion, despite its significant influence in masking damage. In fact, since the damage tends to nucleate and propagate in the most highly stressed zone of the structure, if this zone is near the boundary (e.g. the area close to the clamped section of a cantilever) than the maximum WT coefficients due to the edge effects will mask the damage, leading to situations of false indication or even of false alarm. Spanos et al. [16] considered multi-damaged Euler-Bernoulli beams subjected to static loads and numerically showed that applying the WT on the difference between the damaged and the undamaged beam responses, boundary effects are eliminated and damage-related to local maxima are clearly identified. Rucka and Wilde, imposing the local continuity of the first and second derivatives at the ends, extended the signal outside its original support through a simple cubic spline extrapolation based on three [9] or four [10] neighbouring points. On the other hand, Messina in [17] discusses extensively the border distortion in CWT dealing with the first four Gaussian wavelets and proposed two methods. The first method consists of padding the signal through isomorphisms (called "Rotation" – corresponding to a polar-like symmetry - and "Turnover" – corresponding to a mirror symmetry) of the original signal. The author examined their quality in limiting the border distortions with respect to the beam boundary conditions and the derivative order. The second method (called "Self-minimization") aims at correcting a first approximated extension (e.g. obtained by a fitting polynomial) by minimizing an objective function which depends on the convolution results.
In the present paper, the problem of the damage masked by CWT border distortions is discussed and a new signal extension polynomial method to enhance damage detection by spatial CWT is proposed. The method is based on high-order polynomial functions that fit the original data and its first derivative so as to extend smoothly the signal and its derivatives. To illustrate the effectiveness and the versatility of the method with respect to different boundary conditions and beam deflections (described by either trigonometric or polynomial functions), the free vibrations and the static deflection of a cracked cantilever, and the free vibrations of a cracked simple supported beam are numerically simulated. A synthetic Gaussian white noise is added to the signal to represent real measured data. The fourth order Coiflet basis function is used in wavelet analysis. The method is compared with the traditional linear padding method and with Messina's isomorphism methods.

2. MODELLING OF THE CRACKED BEAM

A cracked Euler-Bernoulli beam characterized by an open edge crack under different boundary conditions at the two ends, i.e. clamped-free (cantilever beam) and supported-supported (simply supported beam), is considered (Fig. 1). The free vibration response of both cantilever and simply supported beams as well as the static deflection of the cantilever beam due to the point load F are analytically evaluated solving the free vibration equations or the static equilibrium equations of the two uncracked sub-beams connected by a rotational spring (representing the local stiffness k_c of the cracked cross-section of the beam) at the crack location, x_c. The beam has a rectangular cross-section with height h and width b; the crack depth is a and L is the beam length. The symbols I, A, E

and ρ represent respectively, moment of inertia and area of the cross-section and Young modulus and density of the material.

Figure 1

2.1. Free vibration

The free vibration response of the two uncracked parts of the beam can be written as

$$EI\frac{\partial^4 v(x,t)}{\partial x^4}+\rho A\frac{\partial^2 v(x,t)}{\partial t^2}=0 \tag{1}$$

where $v(x, t)$ is the transversal displacement of the beam from its static equilibrium position at a distance x from the left end at the time t. Separating the variables in Eq. (1) ($v(x,t)=\eta(x)\,g(t)$) and solving the characteristic equation function of x, the mode shapes η_L and η_R of the left and right sub-beam respectively, are as follows

$$\eta_L = C_{1L}\sin(\alpha x)+C_{2L}\cos(\alpha x)+C_{3L}\sinh(\alpha x)+C_{4L}\cosh(\alpha x) \quad 0\le x<x_c \tag{2.1}$$

and

$$\eta_R = C_{1R}\sin(\alpha x)+C_{2R}\cos(\alpha x)+C_{3R}\sinh(\alpha x)+C_{4R}\cosh(\alpha x) \quad x_c\le x\le L\,. \tag{2.2}$$

where $\alpha=\left(\frac{\rho A\omega^2}{EI}\right)^{1/4}$ and ω is the natural frequency of the cracked beam.

The $C_{(.)}$ terms are integration constants arising from the solution of a fourth order differential equation in space. By imposing the boundary conditions (Eqs. 3) a system of eight linear equations is formed. The natural frequencies of the cracked beam are found by setting the determinant of the matrix of the linear system to zero, and solving it numerically for the roots of α. The coefficient C_{1L} is imposed to be equal to unity.

The boundary conditions of the cantilever beam at the clamped and at the free end are, respectively:

$$\eta_L(0)=0 \quad \text{and} \quad \eta_L'(0)=0\,, \tag{3.1}$$

$$\eta_R''(L)=0 \quad \text{and} \quad \eta_R'''(L)=0\,. \tag{3.2}$$

While the boundary conditions of the simple supported beam at the two ends are:

$$\eta_L(0)=0 \quad \text{and} \quad \eta_L''(0)=0\,, \tag{3.3}$$

$$\eta_R(L)=0 \quad \text{and} \quad \eta_R''(L)=0\,. \tag{3.4}$$

For both the structures, the conditions of continuity of displacement, moment and shear at the crack location can be expressed as

$$\eta_L(x_c)=\eta_R(x_c)\,,\quad \eta_L''(x_c)=\eta_R''(x_c) \quad \text{and} \quad \eta_L'''(x_c)=\eta_R'''(x_c)\,. \tag{3.5}$$

The rotational spring at the cracked section introduces a discontinuity of the rotation, which can be written as

$$\eta_R'(x_c)-\eta_L'(x_c)=\frac{EI}{k_c}\eta_R''(x_c)\,. \tag{3.6}$$

The local stiffness k_c due to the crack is evaluated, according to linear elastic fracture mechanics concepts, through the following expression [25]

$$k_c = \frac{bh^2 E}{24\left(\delta/(1-\delta)\right)^2 (5.93 - 19.69\delta + 37.14\delta^2 - 35.84\delta^3 + 13.12\delta^4)}. \quad (4)$$

where $\delta = a/h$ is the relative crack depth.

2.2. Static deflection

The static deflection of the cracked cantilever subjected to a concentrated force, *F*, at the free end (*x*=*L*), can be modeled starting from the second order static equilibrium equation of the sub-beams at the left and right sides of the cracked section

$$\frac{d^2\eta(x)}{dx^2} = \frac{M(x)}{EI}. \quad (5)$$

where *M*(*x*), the bending moment along the beam due to the force *F*, is equal to $F(L-x)$. Imposing the boundary conditions described in Eqs. (3.1, 3.2, 3.5 and 3.6), the analytical solution of the problem becomes

$$\eta(x) = \frac{F}{EI}\left(\frac{Lx^2}{2} - \frac{x^3}{6}\right) \quad 0 \le x < x_c \quad (6.1)$$

and

$$\eta(x) = \frac{F}{EI}\left(\frac{Lx^2}{2} - \frac{x^3}{6}\right) + \frac{F(L-x_c)}{k_c}(x - x_c) \quad x_c \le x \le L \quad (6.2)$$

3. DAMAGE DETECTION BY SPATIAL CWT

3.1. Wavelet analysis

Thanks to its multi-resolution properties, wavelet analysis, acting as a signal microscope, has the ability to analyze non-stationary signals in more detail than traditional analysis tools, such as Fourier transform or Short-Time Fourier transform.

A wavelet function $\psi(x)$ is a zero mean local wave-like function which decays rapidly, and which satisfies particular conditions [4]. A family of wavelet functions may be obtained by considering:

$$\psi_{k,s}(x) = \frac{1}{\sqrt{s}}\psi\left(\frac{x-k}{s}\right), \quad (7)$$

where *s* and *k* are, respectively, the scale and the translation parameters. The continuous wavelet transform of a signal $\eta(x)$ with respect to the wavelet function $\psi(x)$ is defined as

$$W(k,s) = \int_{-\infty}^{+\infty} \eta(x)\frac{1}{\sqrt{s}}\psi^*\left(\frac{x-k}{s}\right)dx \quad (8)$$

where ψ^* is the complex conjugate of ψ.

Since the identification of a discontinuity in a function or in any of its derivatives can be linked to the number of vanishing moments of the analyzing wavelet function [7], it is possible for a wavelet transform to detect singularities in a signal or its derivatives by choosing an appropriate basis

function $\psi(x)$. Since the presence of an open crack in a beam may introduce a singularity in the derivatives of the deflected shape, wavelet transforms are considered to be a powerful tool to locate the damage. Due to the presence of the singularity, a transformed deflected shape yields a local variation or extremum in the wavelet coefficient at the location of damage throughout the different scales. Wavelet functions with a high number of vanishing moments are appropriate for damage identification purposes, such as the 4^{th} order Coiflets ('Coif4') and the 8^{th} order Symlets ('Sym8'), which both have 8 vanishing moments. Following the suggestion of Pakrashi et al. [7], the 'Coif4' basis function is used throughout the present work. A MATLAB routine to perform the CWT with 'Coif4' has been implemented by the authors to improve the accuracy of the existing MATLAB procedure (the built-in routine approximates the signal thorough a constant piecewise function, while that implemented in this study considers a piecewise linear trend).

3.2. Edge effects and signal extension

As mentioned above, the continuous wavelet transform is defined by the convolution of the input signal, $\eta(x)$, with a wavelet function generated from the mother wavelet, $\psi(x)$, by scaling and translating it. For a finite-length signal, when the convolution operation is executed close to the signal ends, the wavelet window extents into a region with no available data, so that the transform values close to the borders of the signal are tainted by the non-existing data. Consequently, the values of the CWT coefficients very close to the signal extrema arise abnormally (border distortions) and the real signal features of that region are consequently corrupted by the transform. So edge effects can provoke the masking of the damage and yield false indicators (see Section 4).
Among the different approaches to handle edge effects, the most commonly used one is to preprocess the signal through extrema extension [4,18]. Traditional extension techniques include extension by zero padding, periodicity, symmetry and linearization [20]. These methods make simple assumptions about the signal characteristics outside the borders but they prove unsatisfactory for many applications [21-24], including damage detection [9-10,17].
According to the cracked beam model of Section 2, a damage introduces a discontinuity (jump) in the rotation, $\eta'(x)$, of the structural response and consequently a singularity in the curvature, $\eta''(x)$, and in the subsequent derivatives. As is well-known [7], a wavelet with m vanishing moments detects the local discontinuities of the signal and of its derivatives up to the mth order. Therefore, padding functions to be added at either end of the original signal, need to have specific smoothness features to avoid introducing edge discontinuities into the padded signal or its derivatives up to the mth order. The traditional padding methods cited above introduce discontinuities at the ends of the signal and/or in its 1st or 2nd derivatives, so that small damages close to the beam extrema are masked by CWT border distortions. Hence, an ad-hoc extension method that minimizes edge effects must be employed for effective damage detection through wavelet analysis.

3.3. The proposed padding method

Realistic situations where noise is superimposed on the original signal are considered in the following. As a matter of fact, the ideal situation in the absence of noise has a trivial solution as by extending the signal, $\eta(x)$, through its interpolating spline, the border distortions are suppressed and the location of very tiny damages close to the edges are always identified by WT. It is also noted that in the absence of noise WA is not necessary to detect the damage position since by numerically calculating the second derivative of the original signal, the damage location can be readily identified [26]).

The presence of noise is introduced by adding a synthetic Gaussian white noise to the original response. To quantify the noise level, the signal to noise ratio (SNR) is considered. The SNR, expressed in decibels, is defined as

$$SNR = 10\log_{10}\left(\frac{P_{signal}}{P_{noise}}\right). \tag{9}$$

The term P with the subscripts in Eq. (9) denotes power and is computed as

$$P_{(.)} = \frac{1}{N_z}\sum_{i=0}^{N_z-1}\left|z(x_i)\right|^2, \tag{10}$$

where N_z denotes the number of discrete points of a generic sampled function $z(x)$. Note that different measurements of the noise can be adopted. For instance by considering a signal-to-noise ratio SNR* defined as $10\log_{10}\left(\max_{signal}/\sigma_{noise}\right)$ ($\max_{signal}$ = maximum absolute value of the signal, σ_{noise} = standard deviation of the signal), we have: SNR=120dB corresponds to about SNR*=63dB, SNR=100dB corresponds to about SNR*=53dB and so on.

It can be shown, through numerical experiments, that approaches to extend the noisy signal either through its interpolating spline or its fitting spline (as suggested in [9-10]) prove not to be effective. Therefore, a simple and computationally efficient method based on using two polynomial functions $f_1(x_1)$ and $f_2(x_2)$ to extend, in the range $x \le 0$ and $x \ge L$, respectively, the signal $\eta(x)$ is proposed (Fig. 2). These functions are obtained by a fitting procedure in order to:

(i) describe correctly $\eta(x)$ in such a way to extend smoothly the trend of the signal and of its derivatives up to the order equal to the *m*th vanishing moment of the adopted wavelet;

(ii) ensure continuity at the boundaries up to *m*th derivative order.

Since the original signal is corrupted by noise, conditions (i) and (ii) may only be satisfied in an average sense.

When adopting the 'Coif4' wavelet with 8 vanishing moments, boundary continuities up to the 8th derivative of $\eta(x)$ have to be satisfied. Hence, polynomial functions of degree 8 are generated for $f_1(x_1)$ and $f_2(x_2)$.

To define the extension functions, firstly the original noisy data, $\eta(x)$, are fitted in a least squares sense through two polynomial functions $\bar{f}_1(x_1)$ and $\bar{f}_2(x_2)$ as

$$\bar{f}_1(x_1) = \overline{A}_1 x_1^8 + \overline{B}_1 x_1^7 + \overline{C}_1 x_1^6 + \overline{D}_1 x_1^5 + \overline{E}_1 x_1^4 + \overline{F}_1 x_1^3 + \overline{G}_1 x_1^2 + \overline{H}_1 x_1 + \overline{I}_1 \quad \text{with} \quad 0 \le x_1 \le \beta_1 L \tag{11.1}$$

and

$$\bar{f}_2(x_2) = \overline{A}_2 x_2^8 + \overline{B}_2 x_2^7 + \overline{C}_2 x_2^6 + \overline{D}_2 x_2^5 + \overline{E}_2 x_2^4 + \overline{F}_2 x_2^3 + \overline{G}_2 x_2^2 + \overline{H}_2 x_2 + \overline{I}_2 \tag{11.2}$$

with $-L(1-\beta_2) \le x_2 \le 0$,

where $\bar{A}_1, \bar{B}_1, \ldots, \bar{I}_1$ and $\bar{A}_2, \bar{B}_2, \ldots, \bar{I}_2$ are the coefficients of the fitting polynomial functions, $\bar{f}_1(x_1)$ and $\bar{f}_2(x_2)$, respectively. The function $\bar{f}_1(x_1)$ fits $\eta(x)$ from $x = 0$ to $x = \beta_1 L$; while $\bar{f}_2(x_2)$ fits $\eta(x)$ from $x = L(1-\beta_2)$ to $x = L$, where β_1 and β_2 can vary in the range $0.1-1$. There are not optimal values for these parameters, as they depend on the trend of the signal and the noise level. For instance in the case of signals characterized by no sign change of first derivative, values in the range of $0.7-1$ work well while for oscillating signals values in the range $0.1-0.4$ are suggested; moreover the latter values are preferred in the presence of low noise content (see Section 4).

The extension polynomials $f_1(x_1)$ and $f_2(x_2)$, having the same degree of the fitting functions, are

$$f_1(x_1) = A_1 x_1^8 + B_1 x_1^7 + C_1 x_1^6 + D_1 x_1^5 + E_1 x_1^4 + F_1 x_1^3 + G_1 x_1^2 + H_1 x_1 + I_1 \quad \text{with } -\Lambda s \le x_1 \le 0 \tag{12.1}$$

and

$$f_2(x_2) = A_2 x_2^8 + B_2 x_2^7 + C_2 x_2^6 + D_2 x_2^5 + E_2 x_2^4 + F_2 x_2^3 + G_2 x_2^2 + H_2 x_2 + I_2 \text{ with } 0 \le x_2 \le \Lambda s \tag{12.2}$$

where s is the scale parameter considered in the WA, Λ represents the distance from the mother wavelet center to the position where the wavelet attains negligible values (for 'Coif4', $\Lambda = 11dx$ is assumed, where Δx is the sampling step), and $A_1, B_1, \ldots, I_1$ and $A_2, B_2, \ldots, I_2$ are the polynomial coefficients obtained as follows:

$$A_1 = \bar{A}_1;\ B_1 = \bar{B}_1;\ C_1 = \bar{C}_1;\ D_1 = \bar{D}_1;\ E_1 = \bar{E}_1;\ F_1 = \bar{F}_1;\ G_1 = \bar{G}_1;\ H_1 = \bar{H}_1;\ I_1 = \eta(x=0) \tag{13.1}$$

$$A_2 = \bar{A}_2;\ B_2 = \bar{B}_2;\ C_2 = \bar{C}_2;\ D_2 = \bar{D}_2;\ E_2 = \bar{E}_2;\ F_2 = \bar{F}_2;\ G_2 = \bar{G}_2;\ H_2 = \bar{H}_2;\ I_2 = \eta(x=L) \tag{13.2}$$

Then, the coefficients H_1 and H_2 are optimized against the first derivative $\gamma(x)$ of the padded noisy data, $f_1(x) \cup \eta(x) \cup f_2(x)$, numerically calculated at $x = 0$ and $x = L$ through Richardson's extrapolation [27], which allows a high-order approximation (e.g. $O(dx^8)$, $O(dx^{10})$ or $O(dx^{12})$) of the derivative. An iterative procedure is required since H_1 and H_2 are equal to $\gamma(x=0)$ and $\gamma(x=L)$, respectively, which in turn are functions of H_1 and H_2.

Since differentiating the original signal increases the amount of noise, the above described optimization approach is not effective for the other polynomial coefficients, $A_1, \ldots, G_1$ and $A_2, \ldots, G_2$. Note that the last two equalities of Eqs (13.1) and (13.2) impose the fundamental condition of signal continuity at the two extrema. Furthermore, it has to be underlined that good results can be achieved without performing the optimization procedure related to the first derivative (i.e. by assuming $H_1 = \bar{H}_1$ and $H_2 = \bar{H}_2$) and, in fact, better results could be obtained in some cases, e.g., when the noise level is high. Figures 2-4 show a generic noisy data signal, extended through the proposed polynomial functions $f_1(x_1)$ and $f_2(x_2)$, and its 1st and 2nd derivatives. These figures point out that the conditions (i) and (ii), explained above, are satisfied by the proposed method.

Figure 2

Figure 3

Figure 4

4. ILLUSTRATIVE EXAMPLES

The effectiveness and the versatility of the proposed polynomial padding method in minimizing the CWT border distortions is analyzed by considering the mode shapes and the static deflection of both cantilever and simply supported cracked beams. Since the static deflection of a simply supported beam with a crack close to a support under a mid-span vertical point force coincides with that of a cantilever with a crack close to the free end, only the latter case is analysed in the following.

The method is assessed by considering analytical structural responses having different features (trigonometric function for the mode shapes and cubic polynomial for the static responses) and constraint conditions (clamped, simple supported and free). The results are compared to those obtained by the traditional linear padding method [20] and Messina's isomorphism methods [17], experimented by the present authors to be the most effective padding method available in the literature. Note that the latter methods are chosen instead of the Messina's self-minimization method, as they are found to be comparatively more robust and effective (incidentally, in the conclusions reported in Ref. [17] Messina himself recommends to adopt isomorphism methods).

A cracked beam of length L = 1m and a rectangular cross-section of height $h = 0.05L$ and width $b = 0.5h$, constituted by an elastic linear isotropic material with Young modulus, E = 200 GPa, and density, ρ = 7850 kg/m^3, is considered.

The free vibration responses and the static deflections of the beams, sampled at $\Delta x = 0.001L$ intervals, are determined according to the model of Section 2. Such signals are analyzed through CWT, fixing the relative crack depth, δ, unless otherwise specified, to 2% and varying the crack locations, x_c, and the noise level (synthetic Gaussian white noise is used). The wavelet analyses are executed using the 'Coif4' mother wavelet.

4.1 Free vibration response of a cantilever beam

The normalized first mode shape (maximum deflection equal to unity) of the damaged cantilever beam is analysed using the linear padding method, Messina's method (with the "Turnover" method at the clamped end and the "Rotation" method at the free end [28]) and the proposed method (with the fitting parameters, β_1 and β_2 assumed equal to 1). The crack is located at $x = 0.02L$ from the clamped end. A noise level SNR = 120 dB is assumed.

In Fig. 5a, where the linear padding method is used, a jump in the curvature is evident at $x = 0$. In Fig. 5b, where the "Turnover" method is applied to the clamped end, the continuity of the second derivative at $x = 0$ is fulfilled while a jump of the third derivative is expected. On the other hand, in Fig. 5c, thanks to the proposed polynomial padding, no discontinuities are present in the boundaries and the extending functions are in agreement with the average trend in the curvature $\eta''(x)$. It is worth noticing that, for the selected combination of noise level and damage severity and location, it is not possible to locate the crack by analyzing the curvature plot, and hence a wavelet transform technique is necessary to detect such damage.

Figure 5

Figures 5d-f present zooms on the contour plots of the absolute values of the CWT (from scale 1 to scale 40) of the normalized first mode shape padded using the three methods presented above. In the contour plots, the lighter colors represent high coefficient values, whilst darker colors correspond to low coefficient values (see the color bar on the right of Figs. 5d-f). Since a wavelet with more than one vanishing moment (in our case 'Coif4') associates high coefficient values to the signal discontinuities and since high wavelet scales are able to detect a discontinuity even if the wavelet is not centered on it, the contour plot displays a shape pattern characterized by a central bright cone and a number of adjacent less bright cones, all pointing towards the singularity region.
Since the linear padding method introduces a discontinuity in the second derivative at $x = 0$ (Fig. 5a), high coefficient values arise around that region and the bright cone points towards $x = 0$ (Fig. 5d). The damage location is consequently masked because of the edge effects. Furthermore if only the CWT coefficients related to a given scale were considered (e.g. scale 24 in Fig. 6a), the analysis would locate erroneously the damage at about $x = 0.01L$.
When Messina's method is applied, even if a jump in the third derivative occurs at $x = 0$, crack discontinuity at finer and medium scales can be detected as the contour cones point correctly towards the crack location at $x = 0.02L$ (Fig. 5e). On the other hand, at coarser scales, characterized by narrower bands of lower frequencies, the CWT detects the jump of the third derivative and hence it is unable to locate the damage.
Figure 5f shows that, when the proposed polynomial extension method is used, the central bright cone is characterized by an axis centered to the correct damage location. Therefore crack position can be detected at all CWT scales, leading to unambiguous and more reliable damage identification.

The contour plots of the absolute values of the CWT of the normalized third mode shape of the cracked cantilever beam obtained using Messina's method and the proposed polynomial method are presented in Fig. 6 (the crack is located close to the free end at $x = 0.98L$ and a noise level SNR = 140 dB is imposed). Given the oscillating feature of the mode shape, β_1 and β_2 are assumed equal to 0.2 and 0.333, respectively.
Figures 6a and 6b demonstrate that wavelet analysis fails to detect the damage near the free end when Messina's method is applied. This is a consequence of the fact that the curvature near the free end tends to be null and therefore damage identification is more difficult. The jump in the mode shape third derivative at $x = 0$ due to the use of the "Turnover" padding method is the main discontinuity that 'Coif4' wavelet detects in analyzing the padded signal.
On the other hand, using the proposed polynomial padding method, no discontinuity is present at the extrema of the signal or its derivatives, and no border distortion is generated by the wavelet transform. The bright cones point properly to the damage position (see Figs 6c-d).

Figure 6

4.2 Free vibration response of a simply supported beam

Figure 7 shows the effectiveness of Messina's method (the "Rotation" method is applied at both extrema) and the proposed polynomial method (β_1 and β_2 are equal to 1) in the case of the first

mode shape of a cracked simply supported beam corrupted by noise (SNR = 140 dB). The crack, close to the left support at $x = 0.02L$, is correctly identified through both methods. Note that when applied to zero curvature ends, Messina's method does not introduce a discontinuity in the signal or its derivatives, and hence no border distortion occurs. Note also that the brightest cone of Fig. 7a is shifted at coarser scales to the left with respect to the damage location due to the presence of the mirrored damage at $x = -x_c$.

Figure 7

4.3 Static deflection

The normalized noisy static deflections of the cantilever beam subjected to the point load F of Fig. 1, with an open crack of relative depth $\delta = 2\%$, located at $0.02L$ or at $0.098L$, are analysed by CWT. The polynomial extension method is applied assuming β_1 and β_2 equal to 1 and compared with Messina's method. It is observed that even if $\eta(x)$ is a cubic function and the continuity of $\eta(x)$ and its derivatives at the boundaries can be satisfied by polynomial functions of degree three, the presence of noise requires extending polynomial functions in general of eighth order to overcome edge effects.

Both methods prove to be effective in analyzing static deflection when the crack is close to the clamped end (Fig. 8) or when it is near the free end (Fig. 9).

Considering a noise level of SNR = 100 dB, since finer scales are more sensible to noise than coarser ones, the lower parts (from scale 1 to 20) of the CWT contour plots in Figs. 8a and 8c provide somewhat ambiguous damage detection for both considered methods. On the other hand, by considering the upper parts of these contour plots, (from scale 20 to 40), the damage location can clearly be identified (Figs. 8b and 8d).

Figure 8

Fig. 9 compares the effectiveness of the two methods in removing edge effects as the noise level increases. When noise level is at SNR = 100 dB, the damage is clearly located by both methods. Increasing the noise level to SNR = 90 dB the damage is partially masked, while at SNR = 80 dB, the noise completely masks the damage. This behavioral trend demonstrates that CWT border distortions are effectively suppressed by both methods, but damage is masked when a certain level of noise (which is dependent on the specific beam features and damage location and severity) is present.

Figure 9

4.4 Summary of padding method comparison

The linear padding method, Messina's isomorphism methods and the proposed polynomial extension method are qualitatively compared in Figure 10 for a range of mode shapes and static deflections obtained by varying the crack depth ($\delta = 0.0001 - 0.9$) and its location ($x = 0.02L$ or $x = 0.98L$) (see Fig. 10). Crack depth is incremented by $d\delta = 10^{-j-2}$ throughout the range $10^{-j-1} < \delta \le 10^{-j}$ where $j = 0,1,2,3$. For a given noise level, the identification criterion considers that the damage is correctly detected if the highest absolute value of the CWT at the scale 24 falls exactly at the crack location with each of 25 different noise random distributions. Figure 10 identifies the minimum crack depth sizes correctly identified by each method with a given SNR. In these analyses, the fitting parameters β_1 and β_2 equal 1, except in the analysis of the second mode shape of the cantilever beam, where $\beta_1 = 0.15$ and $\beta_2 = 0.125$, and the first mode shape of the simply supported beam, where $\beta_1 = \beta_2 = 0.1667$. Moreover for the second mode shape of the cantilever beam, the values $H_1 = \overline{H}_1$ and $H_2 = \overline{H}_2$ are employed as coefficients of the extension polynomial function.

Figure 10 clearly shows, for all the conditions analysed, the weakness of the linear padding method in tackling border distortions. For instance, when the first mode shape of the cantilever beam with $x_c = 0.98L$ is analysed, even cracks of about $\delta = 0.9$ are masked by edge effects. Moreover, at a given noise level, the minimum crack size that can be identified using the linear padding method is larger than those that can be detected using the other methods. For both the linear padding method and Messina's method, the plots in Figure 10 display plateau representing the minimum crack size that can be correctly detected irrespective of SNR. In the linear padding method this plateau occurs because 'Coif4' recognizes the dominance of the discontinuity in the second derivative at $x = 0$ over the discontinuity introduced to the first derivative by the crack. The crack size identified by the plateau is the smallest that can be identified in this particular structure. As expected, at higher noise levels, the minimum damage that can be detected increases.

With Messina's method, the observed plateaus in the δ-SNR curves are attributable to the discontinuity in the third derivative at $x = 0$ related to the "Turnover" method. Since a jump in the third derivative has less influence on the CWT than one in the second derivative, the smallest crack detectable using Messina's method at a given SNR is smaller than that detectable using the linear padding method. When Messina's method is applied to the mode shapes of the simply supported beam, the minimum identified δ decreases monotonically with increasing SNR (Fig. 10d). As mentioned above, this is due to the fact that the "Rotation" method applied to zero curvature ends does not yield edge discontinuities in all the signal derivatives. With damage at $x = 0.98L$ in a cantilever beam, Messina's method is much more effective when applied to the static deflection than to the first mode shape (see Figs. 10f and 10c). This arises because the first to the mth derivatives of mode shape are all non-zero whilst the derivatives of the cubic static deflection are null from the 4th. As 'Coif4' analyses high order derivatives, the weight of the jump in the third derivative at $x = 0$ is more substantial in the mode shape.

The proposed polynomial padding method is observed to be the most effective and versatile method in analyzing different structural responses corrupted by different noise amounts. At severe noise levels, the proposed polynomial method and Messina's method succeed in identifying very similar

minimum damage levels. However, at medium-to-low noise levels, the polynomial method is more successful in removing CWT border distortions, and is capable of identifying smaller cracks than either of the other methods.

Figure 10

The results being presented in Fig. 10 for a sampling interval $\Delta x = 0.001L$ seem to be confirmed by taking a larger value of the sampling interval. For instance, the same damage identification capacity obtained in the above with $\Delta x = 0.001L$ can be attained by considering a larger sampling interval, provided that a smaller wavelet scale is chosen (the need for a smaller wavelet scale as the sampling interval gets larger is discussed in Ref. [29]). Figure 11 presents the minimum detectable crack size as a function of the signal-to-noise ratio SNR for the first mode shape, sampled at $\Delta x = 0.01L$, in a cantilever beam with crack at $x_c = 0.02L$. The trends turn out to be similar to those reported in Fig. 10a for $\Delta x = 0.001L$.

Figure 11

5. CONCLUSIONS

When wavelet analysis is employed in vibration-based structural damage identification, the issue of border distortions is often crucial as it tends to mask damage near the edges of the structure where high stress levels are liable to occur. Since traditional padding methods are not satisfactory when small near-edge damages need to be detected, an effective and computationally efficient signal extension method is proposed to enhance damage detection by CWT. The method is based on the approach of padding the original signal using two functions that satisfy continuity conditions and extend the average trend and derivatives of the noisy signal. The two high degree polynomial functions employed are determined by imposing signal and first derivative extrema continuity conditions.

To investigate the effectiveness and the versatility of the proposed padding method, the analytical free vibration and static deflection responses of cantilever and simply supported cracked beams were analysed. Variations in crack depth ratio and position are considered, and synthetic Gaussian white noise is introduced to the signal to emulate real measured data. CWT, applying the linear padding method, Messina's isomorphism methods and the proposed polynomial method, is executed to detect the position of damage in the different structural configurations at different noise levels.

The CWT contour plots in the scale from 1 to 40 are analysed. While the linear padding method is generally poor, failing to identify small- and even medium-sized damage close to the beam ends, Messina's method works much better when the crack is close to the cantilever fixed end or when the sinusoidal free vibration of the simply supported beam is analysed. When applied to cantilever beam mode shapes Messina's method does not perform as well. The proposed polynomial method proved to be the most powerful method in dealing with the full range of structural configurations

and damage considered. In particular, smaller cracks can be identified using the proposed method than with either of the other methods, whose formulations introduce a minimum bound on the crack size that can be correctly detected.

In summary, while damage identification using wavelet-based techniques is still an open challenge in the presence of high noise levels, the proposed signal extension method supports improved detection of small damage near beam edges through the minimization of wavelet transform border distortions.

REFERENCES

[1] H. Sohn, C.R. Farrar, F.M. Hemez, D.D. Shunk, D.W. Stinemates, B.R. Nadler, J.J. Czarnecki, A review of structural health monitoring literature: 1996-2001, Los Alamos National Laboratory, LA-13976-MS, 2004.

[2] Y.J. Yana, L. Cheng, Z.Y. Wua, L.H. Yam, Development in vibration-based structural damage detection technique, Mechanical Systems and Signal Processing 21 (2007) 2198-2211.

[3] J.E. Doherty, Nondestructive Evaluation, in: A.S. Kobayashi (Edt.), Handbook on Experimental Mechanics, Society for Experimental Mechanics Inc, 1987.

[4] S. Mallat, A wavelet tour on signal processing, third ed., Academic Press, New York, 2008.

[5] K.M. Liew, Q. Wang, Application of wavelet theory for crack identification in structures, Journal of Engineering Mechanics 124 (1998) 152-157.

[6] Q. Wang, X. Deng, Damage detection with spatial wavelets, International Journal of Solids and Structures 36 (1999) 3443-3468.

[7] V. Pakrashi, B. Basu, A. O'Connor, Structural damage detection and calibration using a wavelet-kurtosis technique, Engineering Structures 29 (2007) 2097-2108.

[8] A. Gentile, A. Messina, On the continuous wavelet transforms applied to discrete vibrational data for detecting open cracks in damaged beams, International Journal of Solids and Structures 40 (2003) 295-315.

[9] M. Rucka, K. Wilde, Crack identification using wavelets on experimental static deflection profiles, Engineering Structures 28 (2006) 279-88.

[10] M. Rucka, K. Wilde, Application of continuous wavelet transform in vibration based damage detection method for beams and plates, Journal of Sound and Vibration 297 (2006) 536-550.

[11] S. Loutridis, E. Douka, A. Trochidis, Crack identification in double cracked beams using wavelet analysis, Journal of Sound and Vibration 277 (2004) 1025-1039.

[12] Q. Wang, N. Wu, Detecting the delamination location of a beam with a wavelet transform: an experimental study, Smart Material and Structures 20 (2011) 012002.

[13] P.K. Rastogi, Optical Measurement Techniques and Applications, Artech House Inc, Boston, 1997.

[14] B. Trentadue, A. Messina, N.I. Giannoccaro, Detecting damage through the processing of dynamic shapes measured by a PSD-triangular laser sensor, International Journal of Solids and Structures 44 (2007) 5554-5575.

[15] J.M. Henault, M. Quiertant, S. Delepine-Lesoille, J. Salin, G. Moreau, F. Taillade, K. Benzarti. Quantitative strain measurement and crack detection in RC structures using a truly distributed fiber optic sensing system, Construction and Building Materials 37 (2012) 916-923.

[16] P.D. Spanos, G. Failla, A. Santini, M. Pappatico, Damage detection in Euler-Bernoulli beams via spatial wavelet analysis, Structural Control and Health Monitoring 13 (2006) 472-487.

[17] A. Messina, Refinements of damage detection methods based on wavelet analysis of dynamical shapes, International Journal of Solids and Structures 45 (2008) 4068-4097.

[18] A. Mertins, Signal Analysis: Wavelet, Filter Banks, Time-Frequency, Transforms and Applications, Wiley, Chichester, 1999.

[19] Y. Deng, W. Wang, C. Qian, Z. Wang, D. Dai, Boundary-processing-technique in EMD method and Hilbert transform, Chinese Science Bulletin 46 (11) (2001) 954-960.

[20] M. Misiti, Y. Misiti, G. Oppenheim, J. Poggi, Wavelet Toolbox, The MathWorks Inc, 2000.

[21] T. Kijewski, A. Kareem, On the presence of end effects and their melioration in wavelet-based analysis, Journal of Sound and Vibration 256 (5) (2002) 980-988.

[22] H. Su, Q. Liu, J. Li, Alleviating Border Effects in Wavelet Transform for Nonlinear Time-varying Signal Analysis, Advances in Electrical and Computer Engineering 11 (3) (2011) 55-60.

[23] J.R. Williams, K. Amaratunga, A Discrete Wavelet Transform Without Edge Effects Using Wavelet Extrapolation, Journal of Fourier Analysis and Applications 3 (4) (1997) 435-449.

[24] D. Zheng, B.F. Chao, Y. Zhou, N. Yu, Improvement of edge effect of the wavelet time-frequency spectrum: application to the length-of-day series, Journal of Geodesy 74 (2000) 249-254.

[25] H. Tada, P.C. Paris, G.R. Irwin, The Stress Analysis of Crack Handbook, second ed., Paris Production, St. Louis, 1985.

[26] A.K. Pandey, M. Biswas, M.M. Samman, Damage detection from changes in curvature mode shapes, Journal of Sound and Vibration 145(2) (1991) 321-332.

[27] K. Atkinson, An introduction to numerical analysis, Second ed., John Wiley & Sons, New York, 1989.

[28] N.I. Giannoccaro, A. Messina, G. Rollo, A damage detection based o the processing of multiple dynamic shapes through CWTs, Proceedings of The Sixth International Conference on Condition Monitoring and Machinery Failure Prevention Technologies, Dublin, 2009.

[29] L. Montanari, Vibration-based damage identification in beam structures through wavelet analysis, PhD Thesis, Univerity of Parma, 2014.

A PADDING METHOD TO REDUCE EDGE EFFECTS FOR ENHANCED DAMAGE IDENTIFICATION USING WAVELET ANALYSIS

Lorenzo MONTANARI, Biswajit BASU, Andrea SPAGNOLI, Brian M. BRODERICK

Figure captions

Fig. 1 - Cracked cantilever and simply-supported beam models.

Fig. 2 - A generic noisy data signal, $\eta(x)$, is extended smoothly before the start by $f_1(x_1)$ and after the end by $f_2(x_2)$.

Fig. 3 - The 1st derivative of the padded noisy signal is shown. The functions $f_1'(x_1)$ and $f_2'(x_2)$ extend $\eta'(x)$ smoothly.

Fig. 4 - The 2nd derivative of the padded noisy signal is plotted. Increasing the derivative order of $\eta(x)$ leads to an increase of noise. However $f_1''(x_1)$ and $f_2''(x_2)$ follow the average trend of $\eta''(x)$.

Fig. 5 - Curvature and contour plots of the absolute values of the CWT of the normalized first mode shape of a cracked cantilever beam with δ = 2% and x_c = 0.02L, and SNR=120 dB: (a,d) linear padding method; (b,e) Messina's method; (c,f) proposed polynomial padding method.

Fig. 6 - Contour plots of the absolute values of the CWT of the normalized third mode shape of the cracked cantilever beam with δ = 2% and x_c = 0.98L, and SNR=140 dB: (a) Messina's method; (b) zoom of (a); (c) proposed polynomial extension method; (d) zoom of (c).

Fig. 7 - Zoom of the contour plot of the absolute values of the CWT of the normalized first mode shape of the cracked simply supported beam with δ = 2% and x_c = 0.02L, and SNR=140 dB: (a) Messina's method; (b) proposed polynomial extension method.

Fig. 8 - Zooms of the contour plots of the absolute values of the CWT of the normalized static deflection of the cracked cantilever beam with δ = 2% and x_c = 0.02L, and SNR=100 dB: (a,b) Messina's method; (c,d) proposed polynomial extension method.

Fig. 9 - Contour plots of the absolute values of the CWT of the normalized static deflection of the cracked cantilever beam with δ = 2% and x_c = 0.98L, for varying noise levels: (a,b) SNR=100 dB; (c,d) SNR=90 dB; (e,f) SNR=80 dB. The contours (a,c,e) and (b,d,f) are obtained using Messina's method and proposed polynomial extension method, respectively.

Fig. 10 – Comparison of the success of the linear padding method, Messina's method and the proposed polynomial method in identifying damage by CWT at scale 24 for varying SNR. The following structural schemes are analysed: (a,b) cantilever first and second mode shapes, respectively, with x_c = 0.02L; (c) cantilever first mode shape with x_c = 0.98L; (d) simply supported beam first mode shape with x_c = 0.02L; (e,f) cantilever static deflection with x_c = 0.02L and x_c = 0.98L, respectively.

Fig. 11 – Comparison of the success of the linear padding method, Messina's method and the proposed polynomial method in identifying damage by CWT using large sampling interval (Δx = 0.01L) at scale 2 for varying SNR. The results refer to cantilever first mode shape, with x_c = 0.02L.

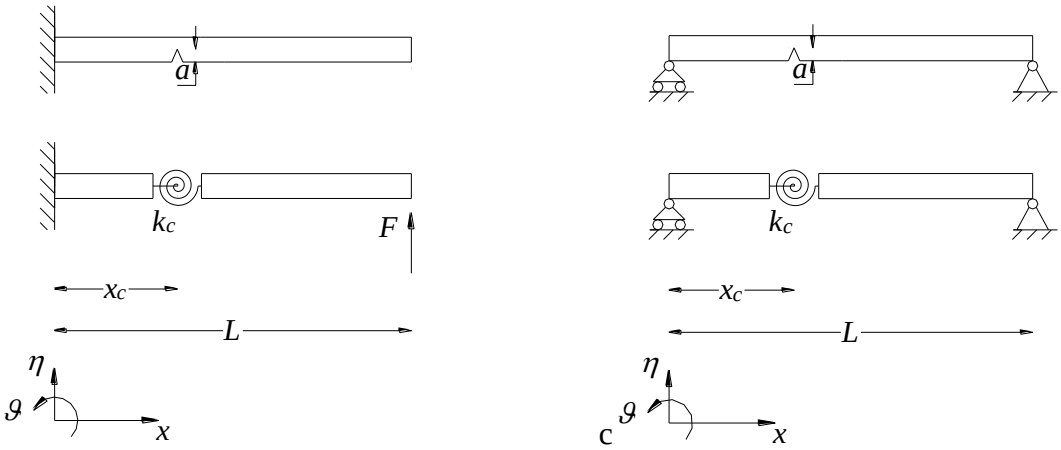

Fig. 1

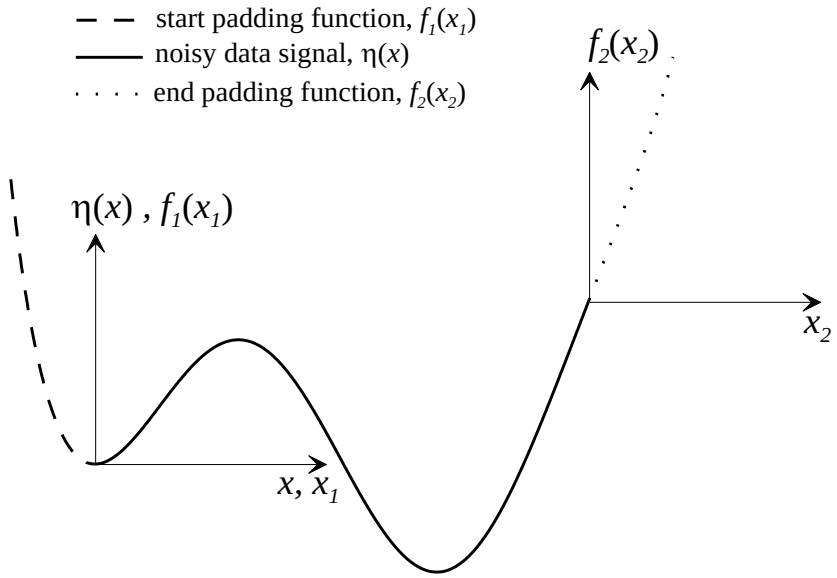
start padding function, $f_1(x_1)$
noisy data signal, $\eta(x)$
end padding function, $f_2(x_2)$
$f_2(x_2)$
$\eta(x)$, $f_1(x_1)$
x_2
x, x_1

Fig. 2

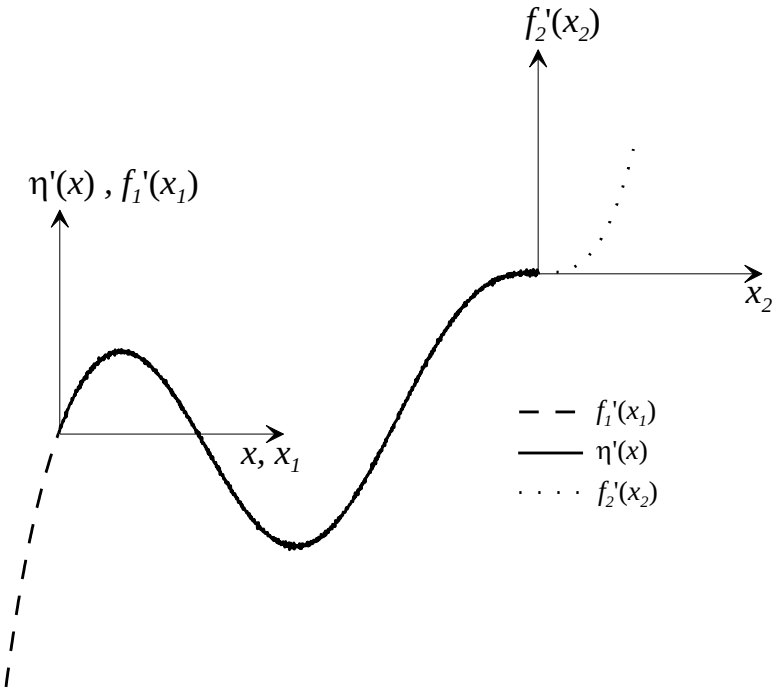

Fig. 3

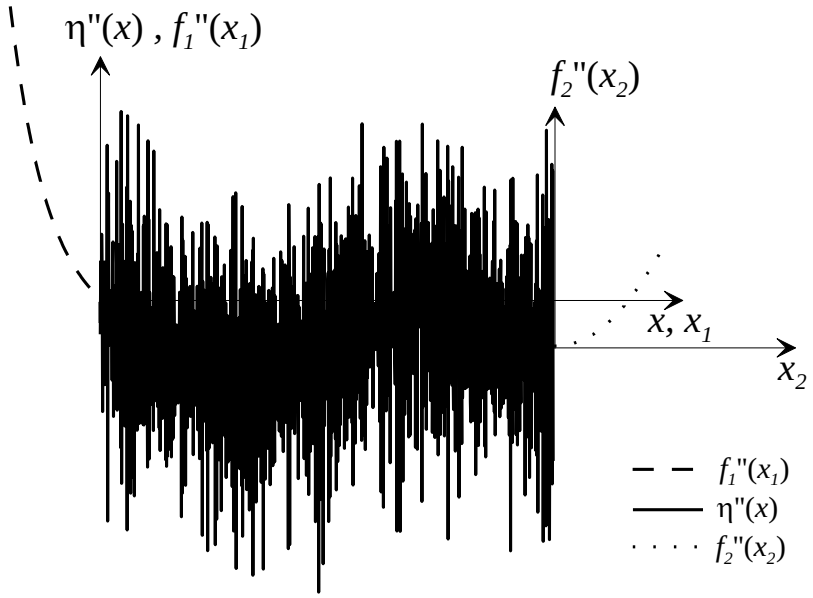

Fig. 4

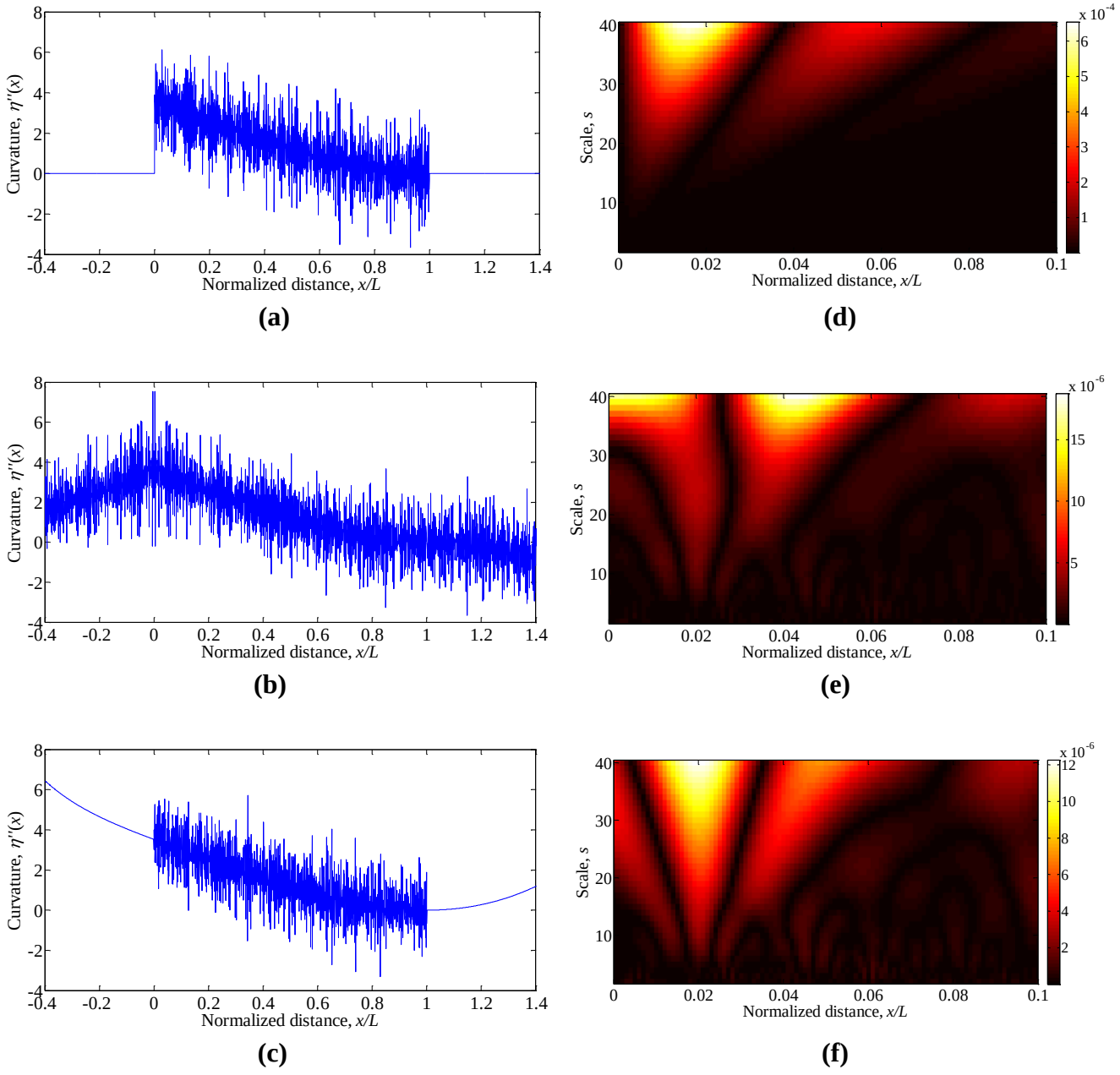
Curvature, η''(x)
Normalized distance, x/L
Scale, s
x 10^-4
x 10^-6
(a)
(b)
(c)
(d)
(e)
(f)

Fig. 5

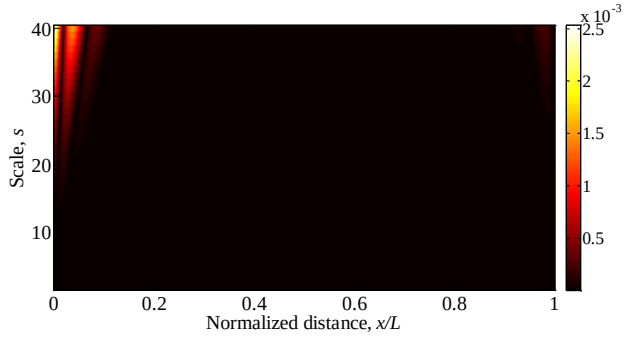
x 10^-3
2.5
2
1.5
1
0.5
40
30
20
10
Scale, s
0
0.2
0.4
0.6
0.8
1
Normalized distance, x/L

(a)

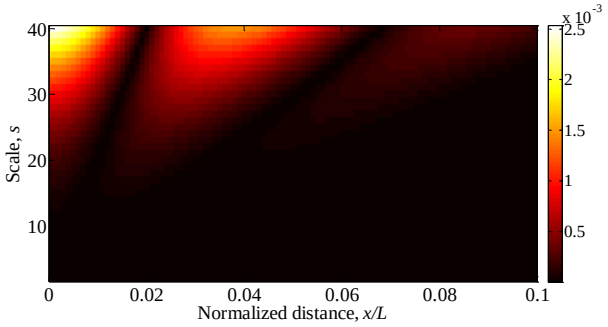
x 10^-3
2.5
2
1.5
1
0.5
40
30
20
10
Scale, s
0
0.02
0.04
0.06
0.08
0.1
Normalized distance, x/L

(b)

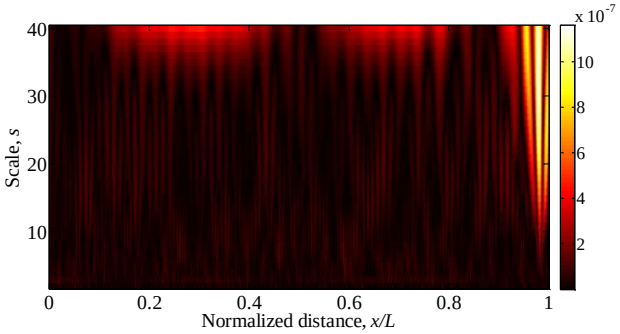
x 10^-7
10
8
6
4
2
40
30
20
10
Scale, s
0
0.2
0.4
0.6
0.8
1
Normalized distance, x/L

(c)

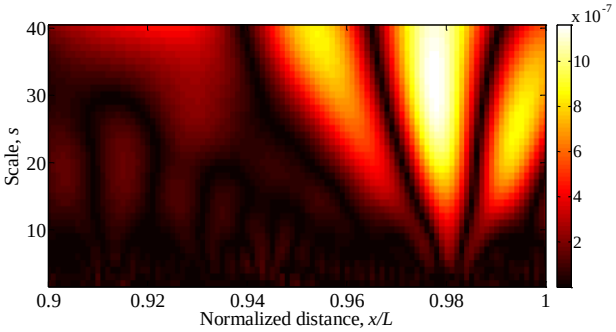
x 10^-7
10
8
6
4
2
40
30
20
10
Scale, s
0.9
0.92
0.94
0.96
0.98
1
Normalized distance, x/L

(d)

Fig. 6

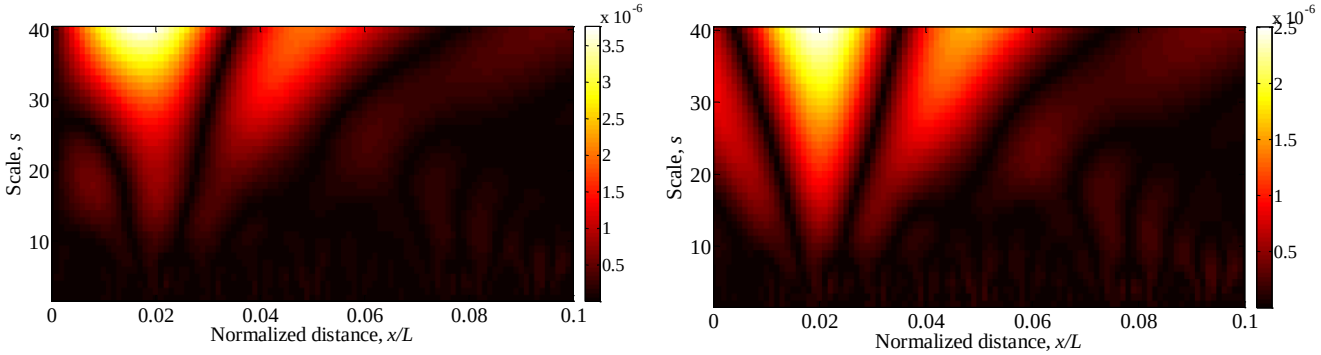
x 10^-6
3.5
3
2.5
2
1.5
1
0.5
40
30
20
10
Scale, s
0
0.02
0.04
0.06
0.08
0.1
Normalized distance, x/L
x 10^-6
2.5
2
1.5
1
0.5
40
30
20
10
Scale, s
0
0.02
0.04
0.06
0.08
0.1
Normalized distance, x/L

(a) **(b)**

Fig. 7

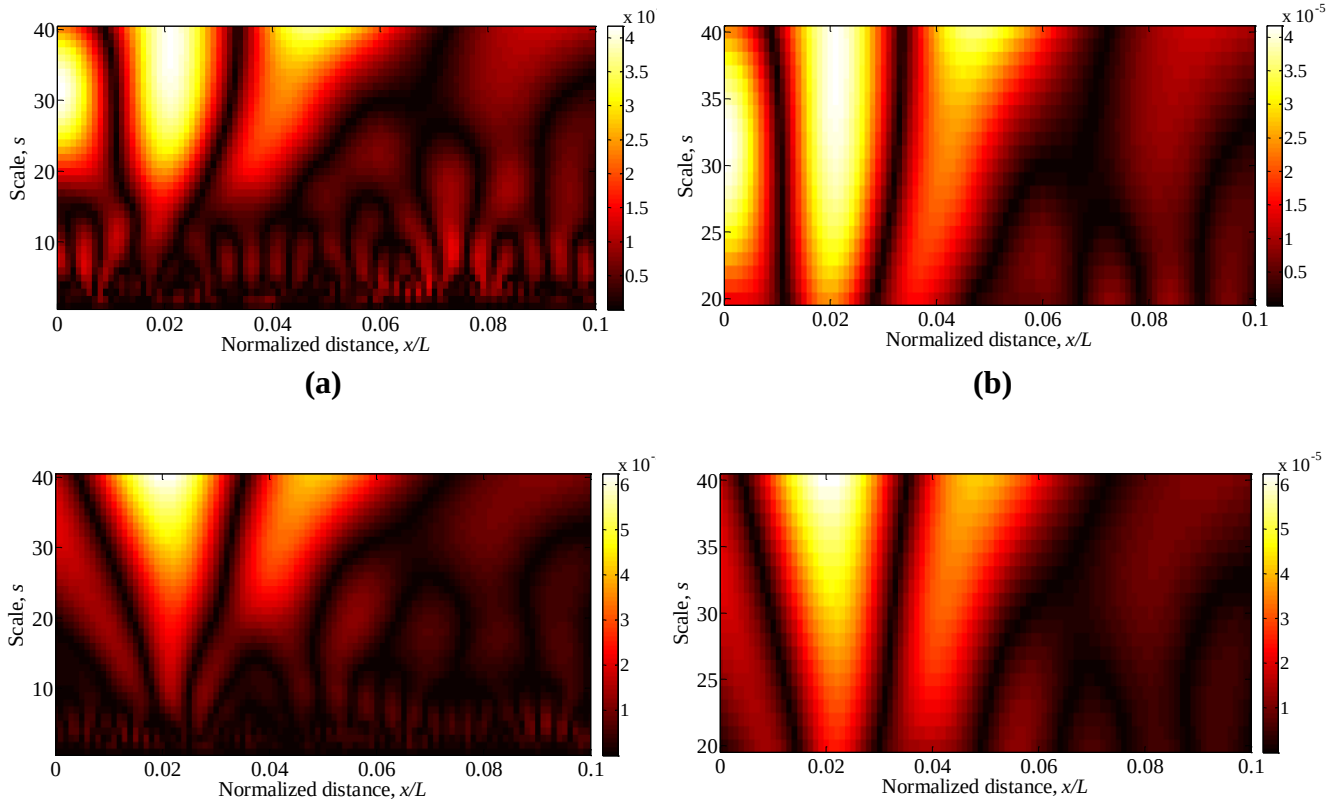
x 10
Scale, s
Normalized distance, x/L
(a)
x 10^-5
Scale, s
Normalized distance, x/L
(b)
x 10^-
Scale, s
Normalized distance, x/L
(c)
x 10^-5
Scale, s
Normalized distance, x/L
(d)

Fig. 8

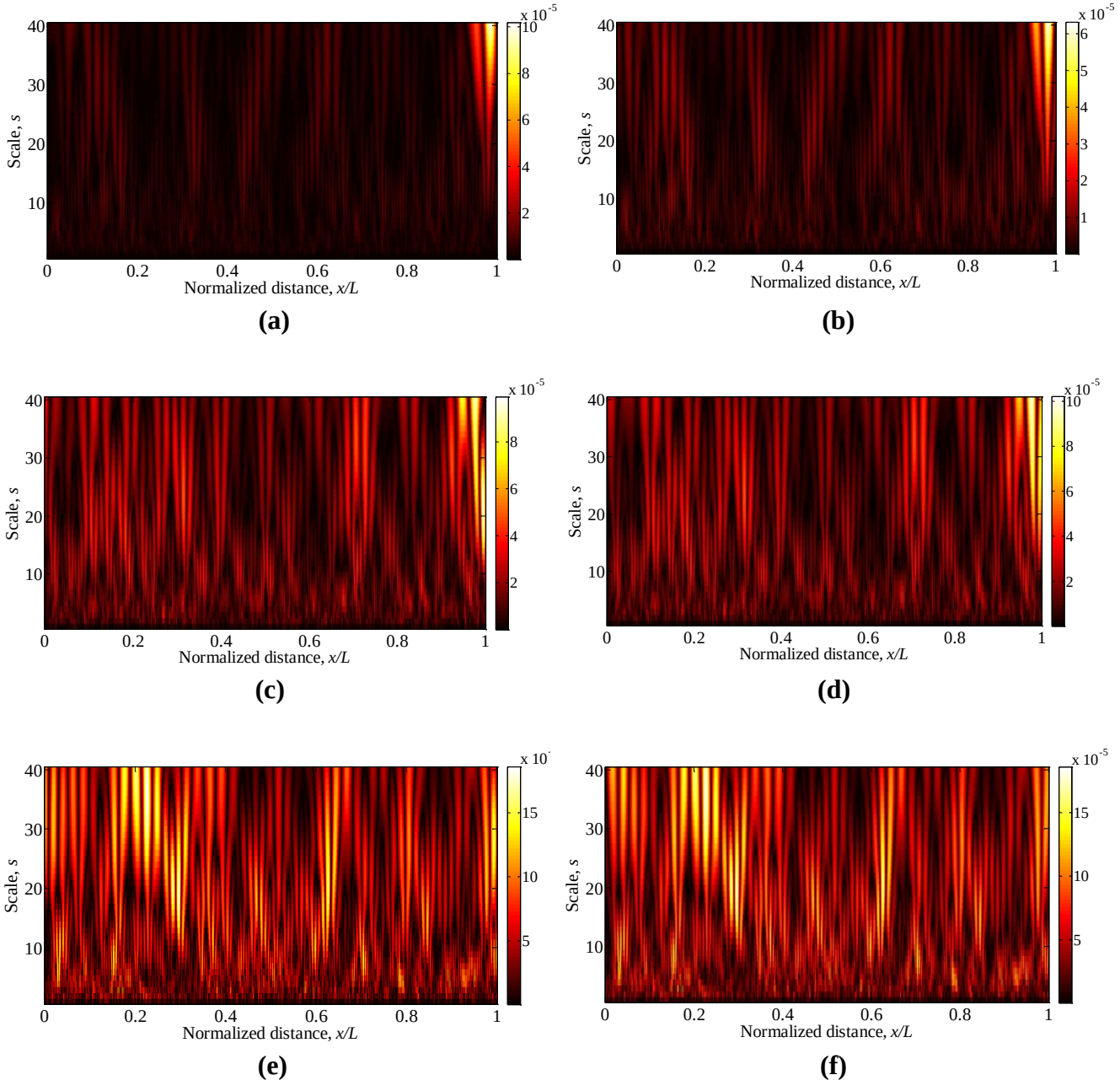

Fig. 9

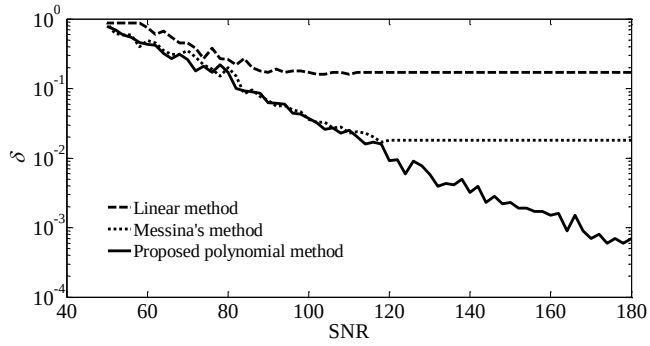

(a)

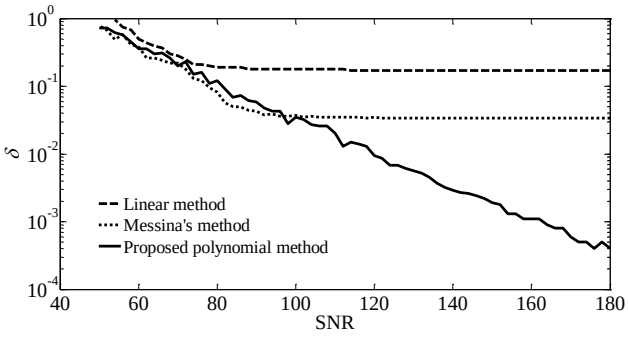

(b)

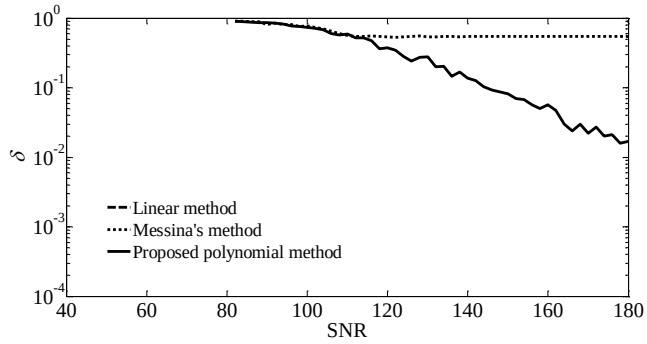

(c)

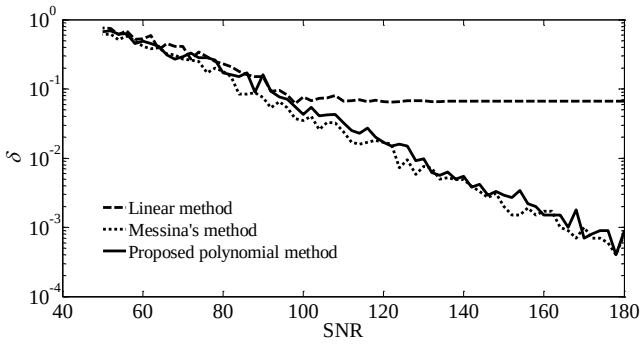

(d)

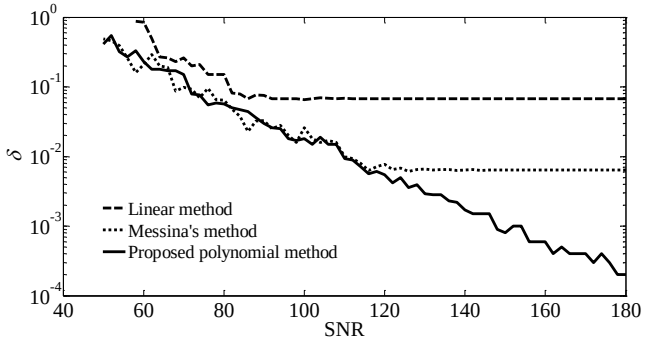

(e)

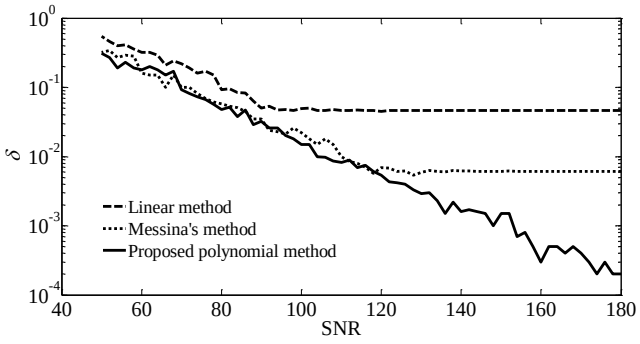

(f)

Fig. 10

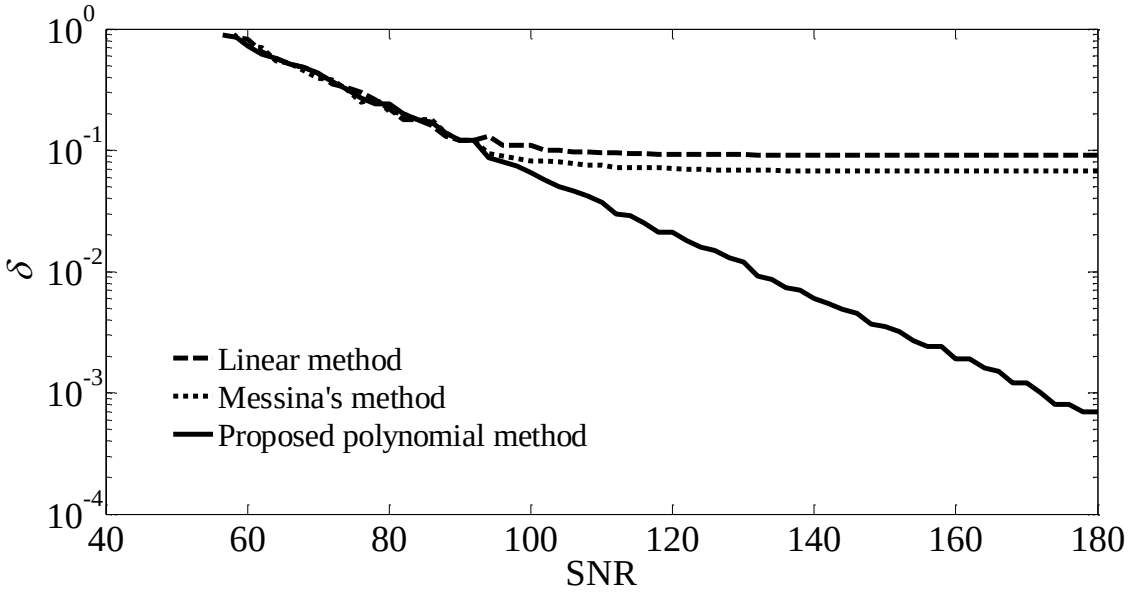
10^{0}
10^{-1}
10^{-2}
10^{-3}
10^{-4}
δ
Linear method
Messina's method
Proposed polynomial method
40
60
80
100
120
140
160
180
SNR

Fig. 11